

UCSF

UC San Francisco Electronic Theses and Dissertations

Title

Ordering the pathway of prion propagation in yeast through a structure/function analysis of Hsp104

Permalink

<https://escholarship.org/uc/item/3ts4v4rc>

Author

Tipton, Kimberly Ann

Publication Date

2008-03-31

Peer reviewed|Thesis/dissertation

Ordering the pathway of prion propagation in yeast through a structure/function
analysis of Hsp104

by
Kimberly A. Tipton

DISSERTATION

Submitted in partial satisfaction of the requirements for the degree of

DOCTOR OF PHILOSOPHY

in
Cell Biology

in the
GRADUATE DIVISION

of the
UNIVERSITY OF CALIFORNIA, SAN FRANCISCO

Copyright (2008)

by

Kimberly A. Tipton

I would like to dedicate this work especially to
F. E. Tipton and R. B. Tipton, who never stopped giving me support and opportunities.

And to the rest of my family: Norlyn, Kathy and Evan, who I hope will be a scientist
someday and say it was because I threw stuff in liquid nitrogen to impress him when he
was six.

ACKNOWLEDGMENTS

This list is very, very long. Longer than what follows and is included for my future remembrance. I want to take a moment to thank the people who I left in Austin, who celebrated my coming here and will celebrate my leaving: Sharon and Harvey Townsend, Charles Kiley, Heather Lloyd and Rachel Hurst. Also John Tesmer, Elizabeth Wyckoff and Shelley Payne for getting me started in science.

It's not completely accurate to say I joined Jonathan Weissman's lab. Rather, I joined Peter Chien's lab, Sean Collins' lab, Angela DePace's lab... these were the people with whom I had daily conversations about science, about getting through graduate school, about our collective experiences good and bad. Peter Chien and Jade Wang were my rotation advisors, and they both gave me a great introduction to the lab and filled in the gaps inevitably left by a busy advisor. I'm especially grateful to have gotten to know Peter and consider him, Holly Field and tiny Liam (who I have yet to meet) among the rare people who become lifelong friends. Sadly, Peter graduated all too soon, but I was fortunate to share years of Weissman lab experiences with our scotch-drinking associate, Sean. Sean's staggering scientific output, scientific input, and idiosyncratic social presence and sense of humor were sources of inspiration, support and delight.

Angela DePace. No one comes near to Angela in the amount of time she spent with me, mostly outside the lab, since she also graduated soon after I joined. I'm proud to call her one of my closest friends and know that she'll transform Harvard Systems Biology with her breadth of perspective, multiplicity of talents and insightful opinions on

the much-neglected art of mentoring. Without her support, my personal and academic life would have been a pale shadow of what it was. And she's really funny.

Jennifer Garrison. Jen singled me out as "different" and another person who took an improbable path in life early in our UCSF careers. She is without a doubt the most thoughtful person I know, and although she is another scientist of amazing talent, what she brought to my life went far beyond scientific insight. I'll never forget the lazy sun-drenched day I spent with Jen and Ami Bhatt in Hayes Valley before they left me for the east coast. Or the bereavement cannelloni.

Ami. The single most hard-working, conscientious and generous person I know, I benefited from her strange wisdom (considering she was one of the very young people of UCSF who otherwise baffled me with their straightforward lives and perspectives) throughout my graduate career. Along with Angela and Jen, I consider Ami a rare find who will always be a part of my life. Thanks so much to all of you.

Clement Chu. Clement is generous to a fault, and I have been on the receiving end of his generosity endlessly within the lab and without. If Clement doesn't know the answer to your question, you can bet he'll be combing through technical literature or websites to find it for you. I've enjoyed sharing many, many dinners with Clement and talking about science and academic social dynamics. And the cats love the tuna guy.

Dale Cameron and Tracy Kress, Cat Foo (who should have turned up sooner to keep me company all these years) and Michael Bassik have become wonderful friends, whom I've shared many a dinner and many a glass of wine or beer with. Jimena Weibezahn brought much-needed AAA+ knowledge and was always willing to discuss my project. Other great sources of support and advice in the lab: Julie Hollien, Maya

Schuldiner, Arunashree Bhamidipati, Vladimir Denic, Lev Osherovich. Thank you all. I owe thanks as well to the three winners of the year of six, as I like to call them: Erin Quan, who was an exceptional rotation student and has developed into a very accomplished scientist, Katie Filaski who has been closer to me project-wise than anyone and has been always willing to help experimentally, and Brandon Toyama, whose initial quiet exterior camouflaged a great experimental craftsman and a diehard foodie.

My committee: David Agard, Dyche Mullins and Carol Gross. I owe all of them deep thanks for counterbalancing the sometimes scattered directions of my project(s) and giving me great advice. Dave turned around my NTD project by advocating structure-based analysis and has been fantastic in advising me about what may come next. Carol brought a calm sagemess to discussions about my current work and about future plans. Dyche has become a good friend as well as a scientific advisor. His style of intellectual inquiry and presentation resonate with me like few others, and I can only hope to be half the scientist that he is.

Other faculty that made an impact on my graduate career: Peter Walter, Dave Morgan, Jeff Cox. All the people who have taken care of the logistics: Alice Willis, Manny, Sue Adams, and Joyce Ramponi are first among many others.

Finally: Jonathan. Jonathan has an endless optimism and takes absolutely nothing personally, at least for more than a minute or two. Which means that every day is a fresh start. His efficient pinpointing of the next question and detailed strategies for solving that question have and will continue to bring him great success. I owe him thanks for continually trying to improve my project and for making my transition to what follows as smooth as possible.

CONTRIBUTIONS

I am deeply indebted to Peter Chien for the origins of my projects in the Weissman lab. His foray into chimera construction was the foundation for my thesis work.

Clement Chu solved the crystal structure of Hsp104 NTD, which allowed me to put the mutants into physical perspective and to identify the most promising sequence divergences. Katie Verges performed the original IPs for 4BAPtrap [*PSI*⁺] vs. [*psi*⁻] and constructed the ClpP reagents I used to make my strains. She also performed experiments exploring the ability of 4BAP to maintain [*RNQ*⁺] and to cure [*PSI*⁺] when overexpressed. Erin Quan identified Q52L in the NTD as a prion-destabilizing mutant during her rotation with me. Recently, Jimena Weibezahn has been a valuable consultant for all things Hsp100.

Several reagents were gifts of Elizabeth Craig and Bernd Bukau. Axel Mogk and Peter Tessarz were helpful in discussing 4BAP and the Hsp104/ClpB chimeras.

ABSTRACT

In these studies, I investigate the role of Hsp104 in the *Saccharomyces cerevisiae* prion propagation pathway by an *in vivo* analysis using synthetic Hsp104 chimera constructs, by mutagenesis of the potentially substrate-recognizing N-terminal domain (NTD) and by extract-based assays of Hsp104 activity.

The yeast prion [*PSI*⁺] is an amyloid-based aggregate of the translation termination factor Sup35 and is strictly reliant upon the Clp/Hsp100 AAA+ ATPase Hsp104 for its maintenance in a dividing cell population. Early extract experiments indicated Hsp104 activity on Sup35 fibers is a severing reaction that results in the production of fiber fragments. Through my synthetic biology experiments, I find that this Hsp104 yeast prion propagation reaction depends upon an initial step mediated by the Hsp40 Sis1, and by extension the Hsp70 Ssa1/2, and proceeds by translocation of prion proteins from aggregated substrates through the central channel of Hsp104. My data indicate there is no necessary downstream coupling of Hsp104 to other yeast chaperone systems for its function in prion propagation. Finally, I identify the mutation R59A in the NTD, which has no effect on amorphous aggregates and has differing effects on distinct conformations of [*PSI*⁺] aggregates. From these findings, I extend my model of prion propagation to include the NTD as an important substrate-selective gate and processivity factor for Hsp104 function.

Jonathan S. Weissman, Ph.D.
Thesis Advisor

TABLE OF CONTENTS

Preface	Acknowledgments	iv
	Contributions	vii
	Abstract	viii
	Table of Contents	ix
	List of Figures	x
Chapter 1	Introduction	1
Chapter 2	Ordering the Pathway of Prion Propagation in Yeast	6
Chapter 3	The N-terminal domain of Hsp104 alters prion variants in yeast	39
Appendix A	Supplementary Information for Chapter 2	61
Appendix B	Hsp104/ClpB chimera function in yeast	65
Appendix C	Hsp104-containing extracts sever Sup35NM fibers	71
Appendix D	References	76

LIST OF FIGURES

CHAPTER 2

Figure 1	Thermotolerance function requires endogenous top ring of Hsp104 and ClpB	12
Figure 2	Prion propagation in yeast relies upon the endogenous top ring of Hsp104	16
Figure 3	444B can be altered to form 4BAP, a protease-coupling Hsp100	19
Figure 4	4BAP translocates prion proteins in an aggregate-dependent fashion	22
Figure 5	$[PSI^+]$ propagation and prion protein translocation depend upon the Hsp40 Sis1	26
Figure 6	Model of Hsp104 cooperation with the Hsp70/40 system in propagating yeast prions	30

CHAPTER 3

Figure 1	NTD of <i>S. cerevisiae</i> conveys prion-specific phenotypes	42
Figure 2	Random and targeted mutagenesis uncovers adjacent loops on the NTD crystal structure important for $[PSI^+]$ modulation	46
Figure 3	NTD mutant R59A shows a strong $[PSI^+]$ phenotype but no defect in luciferase refolding	51
Figure 4	Deletion of NTD strengthens defined variants of $[PSI^+]$, but R59A mutation of NTD affects variants differently	53
Figure 5	Model of the role of NTD in prion propagation	57

APPENDIX A

Figure 1	Expression Levels of Hsp100s in yeast and bacteria	62
Figure 2	Sis1 inhibition reduces translocation of prion proteins from their aggregate substrates	63

APPENDIX B

Figure	Hsp104/ClpB chimera functions in thermotolerance and prion propagation	68
---------------	--	----

APPENDIX C

Figure	Hsp104-containing extracts sever SupNM fibers	73
---------------	---	----

Chapter 1

Introduction

Overview

In this thesis, I present in two major chapters the parts of my graduate work that formed cohesive stories. In Chapter 2, I present an analysis of the domain contribution of Hsp104 to its Hsp70/40-dependent functions in yeast and create a set of tools to monitor prion flux *in vivo*. With those tools, I identify a new component in the propagation cycle of the yeast prion [*PSI*⁺], the Hsp40 Sis1, and determine that Hsp70/40 action occurs upstream of Hsp104 action in prion propagation. In Chapter 3, I present my studies concerning the role of the dispensable N-terminal domain (NTD) of Hsp104 in its actions on amorphous and ordered aggregates. I find that [*PSI*⁺] strength and stability is affected by the presence or absence of the NTD and that NTD mutants can have opposing effects on different [*PSI*⁺] variants. I close both chapters with a model of prion propagation that can now be tested using the materials and strategies I used in my graduate work.

Two independent appendices follow the main text. In Appendix B, I report some preliminary data that shows functioning in a few Hsp104/ClpB chimeras that were not expected to work, and I discuss the implications for Hsp100 general and cell-specific architecture of these results. In Appendix C, I describe an early assay I developed to monitor Sup35 fiber cleavage, which may be useful in some form to future lab members.

I have omitted from the text the various Hsp104 purifications, determination of ATPase activity, gel filtration and sucrose cushion experiments to check assembly and all the data I collected on the non-activity of Hsp104 on Sup35NM fibers. These are helpful only as protocols and have been left in the very capable hands of Brandon Toyama and Katie Verges.

Amyloids

An astonishing variety of proteins have the capacity to form fibrillar aggregates, or amyloid fibers [1]. Formation of these fibers requires a slow nucleation process where natively folded proteins alter conformation and form a “seed” which subsequently can template new monomers in a fast elongation process. Structural studies of many of these aggregates, including fibers formed by Sup35 peptides, increasingly are showing arrangements of β -sheets, stacked such that main-chain interactions hold the “sides” of the individual sheets together and side chains extend toward and intercalate between side chains of a facing β -sheet. Fibrils are formed by sheet-upon-sheet stacking of these units, the long axis of the fibril perpendicular to the “filling” of the tightly packed side chains. Fibrils can then associate laterally to form multi-strand fibers.

These amyloid fibers are extremely stable, being resistant to heat, detergent and other denaturing treatments that easily unfold native proteins and even break up amorphous aggregates. Accumulation of amyloid fibers in tissues is a hallmark of many human diseases, particularly neurodegenerative diseases. Although these fiber deposits are associated with toxicity, it is uncertain whether this is a causative or a correlative effect. The converse to the wide array of proteins being able to form amyloid fibers, each with a strict conformational template, is the phenomenon of a single protein forming many different conformations of amyloid. As research into human disease progresses, we may find that certain conformations of amyloid are more toxic than others, more protective than others or more easily cleared by the body than others. Having a tractable model system to study how amyloid fibers are processed in a cellular context will be a valuable tool to understanding amyloid biology and its implications for human disease.

Yeast Prions

In yeast, amyloid fibers of certain proteins, including the translation termination factor Sup35, form and are inherited in a stable manner. This “infectivity” the Sup35-based [*PSI*⁺] and other yeast aggregates led to the proposal that they were yeast prions [2]. Not all amyloids that form in yeast can become prions, however. Amyloidogenic poly-glutamine tracts form aggregates in yeast, but only with the addition of peptide repeat sequences from Sup35 do they become stably inherited and by definition, prions [3]. The determining factor in whether an amyloid becomes a prion in yeast is whether the cellular machinery can efficiently divide the aggregate to keep up with cell division. In *S. cerevisiae*, the central player in this chaperone-mediated propagation cycle in the AAA+ ATPase Hsp104 [4]. Yeast prions critically rely upon Hsp104 for their maintenance, an action that can be attributed to breaking of the amyloid fiber substrate (Appendix C), [5-7].

Hsp104: Clp/Hsp100 family member

Hsp104 is a member of the Clp/Hsp100 family of protein unfoldases within the larger family of AAA+ ATPase macromolecular remodeling factors [8]. The Hsp100s form hexamers with a central pore through which substrates are threaded to be proteolyzed or refolded. The ability of the Hsp100 to successfully process substrates depends upon recognition steps that are mediated by co-chaperones and adaptors [9], and upon engagement of the translocation machinery, which depends upon the rate of ATP turnover and the stability of the substrate [10-12]. Substrate tag, co-chaperone and

adaptor interactions with the Hsp100s usually occur not through the AAA+ domain but through additional, often N-terminal domains [13-16]. Hsp104 has two AAA+ domains that form a double-tiered hexamer as well as an N-terminal domain (NTD) and a coiled-coil domain (CC), which are attractive candidates for conveying substrate specificity through direct interactions with substrate or, more likely, through interactions with co-chaperones or other factors. Understanding how Hsp104 works on amyloid substrates critically depends upon identifying all of the necessary proteins in the pathway and having a system for monitoring reaction products.

Understanding Hsp104

My studies focused on using chimera approaches to identify domains of Hsp104 that were necessary for $[PSI^+]$ propagation and how they might partner to co-chaperones. I established that the Hsp40 Sis1 was necessary for Sup35 to flux through Hsp104 and for $[PSI^+]$ maintenance. For part of my studies, I concentrated on the NTD of Hsp104 as a candidate for $[PSI^+]$ modulation and have discovered a mutant, R59A, which has differing effects on $[PSI^+]$ variants and no effect on other Hsp104 functions, making it an excellent candidate for physical interaction with fibers. I further developed a system *in vivo* to track prion flux through Hsp104, a system that is promising for *in vitro* studies as well. I have not yet discovered the mechanism of Hsp104 action on Sup35 fibers, but I have laid a foundation for future lab members to do so. Good luck, you guys.

Chapter 2

Ordering the pathway of prion propagation in yeast

Introduction

Protein aggregation is a problem aging, stressed or diseased cells frequently encounter and must address to avert potentially fatal toxic consequences. Of particular interest are unusually stable β -sheet-rich aggregates, or amyloid fibers, formed by a wide array of unrelated proteins and that accumulate intra- or extra-cellularly during the progression of neurodegenerative diseases such as Alzheimer's, Parkinson's and Huntington's. Molecular chaperones are intimately involved in aggregate prevention and dissolution, and their activities can alleviate toxicity associated with protein misfolding in neurodegenerative diseases [17]. How chaperones recognize and act on these particularly recalcitrant aggregates is largely unknown. In yeast, certain proteins form amyloid aggregates that are stably inherited through a prion-like mechanism [2] involving a propagation cycle of fiber growth and chaperone-mediated division. These yeast prions have the potential to serve as a powerful model for generally understanding the action of chaperones on amyloid aggregates in a cellular context.

The yeast prion [PSI^+], caused by amyloid aggregates of the translation termination factor Sup35, is a particularly attractive system for studying chaperone-amyloid biology. Along with the advantages conferred by the use of a simple, well-studied organism, [PSI^+] has a convenient phenotype easily monitored by color. This color phenotype varies in intensity with the severity of the nonsense suppression resulting from Sup35 aggregation. Further, [PSI^+] manifests variants or "strains" with differing strengths and stabilities. Variants are determined by the underlying conformation of the

Sup35 aggregate [18, 19], and their presence allows for the study of how these conformational differences affect the efficiency and nature of chaperone action.

Inheritance of all variants of $[PSI^+]$ critically depends upon particular levels of the chaperone Hsp104 [4]. Deletion of Hsp104 eliminates $[PSI^+]$ as well as all other natural yeast prions, and ectopic overexpression of Hsp104 cures cells of $[PSI^+]$ [4]. This dosage response curve of $[PSI^+]$ to Hsp104 has complicated efforts to study its mechanism *in vivo*. Both inhibition and increased activity of Hsp104 generates more soluble Sup35 and alters the nature of $[PSI^+]$ aggregates. Partially denaturing gel electrophoresis analysis of cell lysates indicates polymers get larger with increasing or decreasing Hsp104 activity [20]. Aggregate size alone is therefore not a reliable reporter of a particular chaperone activity but rather a net effect of complex processes. A more physically proximal reporter of chaperone activity *in vivo* is needed to understand specific actions on amyloid aggregates.

The role of Hsp104 in $[PSI^+]$ propagation is considered to be a fragmentation of the ordered aggregate to expose new surfaces for growth [6], and this activity, as well as aggregate nucleation and reduction of amyloids to noninfective aggregates, has been shown *in vitro* for Hsp104 on Sup35 [7, 21]. It is not clear which of these actions of Hsp104 are necessary for the prion propagation cycle *in vivo*. Although Hsp104 was shown to accelerate the formation of amyloid fibers from Sup35 monomers, chemical inhibition of Hsp104 has no effect on $[PSI^+]$ formation *in vivo* [22]. Further, the ability of Hsp104 alone to efficiently fragment Sup35NM fibers was disputed in a subsequent extract-based study that proposed unknown accessory factors were necessary for this

action [5]. Contributing to the confusion over the relevance of *in vitro* findings of Hsp104 activity are the many *in vivo* studies of the effect of chaperones on $[PSI^+]$.

$[PSI^+]$ is to varying degrees affected by chaperones other than Hsp104, most notably the Hsp70s and Hsp40s [23, 24]. Several mutagenesis studies have implicated Ssa1 in $[PSI^+]$ maintenance [25], with residues affecting the ATPase cycle, peptide binding strength and coupling to the Hsp40s or Hsp90 system especially represented [26-28]. A dominant negative allele of Ssa1 destabilizes $[PSI^+]$ and reduces the number of infective units in the cell [29]. Ssa1 has further been shown to physically interact with Sup35 preferentially in $[PSI^+]$ cells [30], a finding that is intriguingly parallel to the findings that the Hsp40 Sis1 binds aggregates of the yeast prion $[RNQ^+]$ [31, 32]. Sis1 has been demonstrated to be necessary for the maintenance of $[RNQ^+]$ [32] and to modulate the size and infectivity of $[RNQ^+]$ aggregates [33]. The many studies showing chaperones other than Hsp104 modulate $[PSI^+]$ and other yeast prions *in vivo* as well as the lack of clear relevance of Hsp104 studies *in vitro* underscore the need to create a system that monitors the prion propagation cycle in the context of the cell and at a level of precision that can identify and order cofactors in the process.

The implication of the Hsp70/40 system in $[PSI^+]$ propagation *in vivo* is particularly compelling in light of what is known about how Hsp104 and its bacterial homolog, ClpB, act on amorphous aggregates. Hsp104/ClpB are members of the Clp/Hsp100 family, which falls within the AAA+ ATPase superfamily of macromolecular remodeling factors. AAA+ ATPases are defined by the presence of one or more AAA domains, which assemble into hexameric structures containing a central pore through which substrates are threaded in an ATP-dependent fashion. Family

members have evolved accessory N-terminal or other additional domains that modulate the central motor of the hexamer and often interact with co-chaperones, substrates or adaptors [9, 34]. Hsp104/ClpB comprises a two-tiered hexamer (Fig 1a, 1b) with AAA1 preceded by an N-terminal domain (NTD) and interrupted by a long coiled-coil domain (CC) and this entire top tier connected to AAA2 by a small helix [8, 35]. The central action of the Hsp104/ClpB hexamer couples with co-chaperones Hsp70 and Hsp40 to unfold proteins from stress-induced aggregates so they may properly refold [36-39]. The pathway and mechanism of this disaggregation reaction has been more extensively studied for ClpB, with its 70/40 co-chaperones and nucleotide exchange factor, DnaK/DnaJ/GrpE. Mounting evidence indicates the initial step in the disaggregation reaction is mediated by DnaK [40-42], which interacts with the top tier of ClpB [43] to hand off the substrate for translocation through the hexamer [40, 44]. However, it remains unclear whether this order of operations is also true for Hsp104 [45] and whether the Hsp70/40 system couples to the exit of the hexamer to assist substrate refolding. Further, the cooperation of Hsp100s with the Hsp70/40 system is species-specific. Co-evolution of these systems has led to the inability of ClpB to operate with yeast Hsp70/40 or for Hsp104 to operate with DnaKJ [36, 46].

We relied upon these previous studies and our hypothesis of an Hsp100 modular architecture to construct Hsp100 chimeras that would allow us to identify and order components of the natural prion propagation cycle. By replacing the AAA2 of Hsp104 with the homologous sequence from ClpB and testing the resulting chimera in yeast, we show that the Hsp104 AAA2 is dispensable for prion propagation and induced thermotolerance functions. Likewise, AAA2 of ClpB can successfully be replaced by the

Hsp104 sequence in bacteria. By adapting our chimera to couple with a catalytically inactive version of the bacterial peptidase ClpP (ClpP^{trap} or Trap) [40, 47], forming 4BAP, we demonstrate translocation of Sup35 occurs preferentially in [*PSI*⁺] yeast, in agreement with a very recent study [48]. We extended these results to include the [*RNQ*⁺] prion and different variants of [*PSI*⁺] and showed that translocation efficiency depends upon the prion variant. We further show that repression of the Hsp40 Sis1 abrogates translocation through 4BAP and cures HSP104 wildtype cells of [*PSI*⁺]. These results lead us to propose an *in vivo* model of prion propagation that relies upon an obligate upstream step of amyloid aggregate recognition by the Hsp70/40 system and proceeds through translocation of substrate through the Hsp104 pore, yielding a divided aggregate and possibly a soluble Sup35 monomer.

Results

Clp/Hsp100 members have a modular architecture

The successful functioning of an Hsp104/ClpB chimera critically depended upon modularity in Hsp100 architecture that was suggested by phylogeny and structure but not clear operationally. Our first step, then, was to establish that ClpB/Hsp104 chimeras would be active in relevant *in vivo* assays. To construct the chimera, we examined the TClpB structure [49] along with alignments of TClpB, ClpB and Hsp104 and selected as our fusion point a conserved motif (TG/IPV) in a helix connecting AAA1 and AAA2 (Fig 1a, 1b). We named the resulting chimera 444B (Hsp104_{NTD-AAA1-CC} + ClpB_{AAA2}) and its inverse version BBB4 (ClpB_{NTD-AAA1-CC} + Hsp104_{AAA2}).

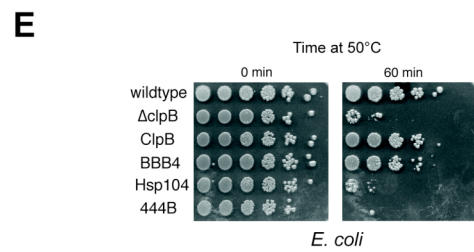
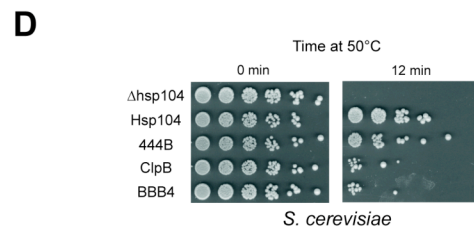
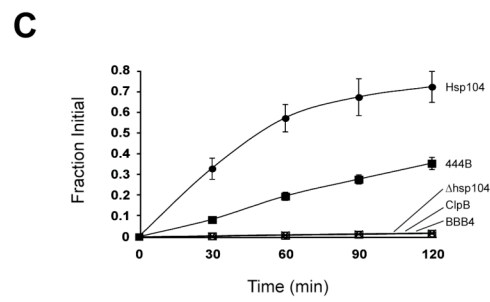
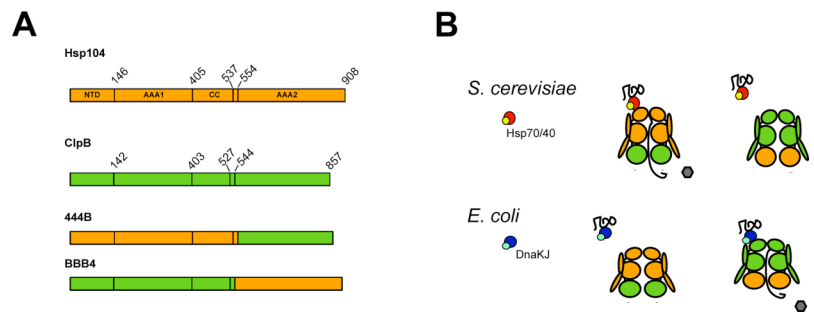


Figure 1. Thermotolerance function requires endogenous top ring of Hsp104 and ClpB.

(A) Diagram of the domain structures of Hsp104 and ClpB and of the chimeras 444B and BBB4. The fusion point TG/IPV occurs at 554 in Hsp104 and 544 in ClpB.

(B) Cartoon schematic of the Hsp104/ClpB chimeras and their predicted interactions with the Hsp70/40 systems in yeast and bacteria.

(C) Luciferase reactivation by Hsp100s in *S. cerevisiae*. HSP104 deletion strains expressing luciferase episomally under the constitutive GPD promoter were transformed with low-copy plasmids encoding the indicated Hsp100 under the control of the HSP104 promoter. Log phase cultures were shifted to 37°C for one hour to induce Hsp100 expression, treated with cycloheximide to halt new protein synthesis, heat shocked at 42°C and allowed to recover at 30°C. Luciferase activity was measured at the indicated times during recovery and plotted as a fraction of pre-heat shock activity levels.

(D) Induced thermotolerance function of Hsp100 constructs in *S. cerevisiae*. Hsp104 deletion strains carrying the indicated Hsp100 under the control of the HSP104 promoter were shifted from 30°C to 37°C at mid-log phase for one hour and subsequently exposed to 50°C. Aliquots were removed at the indicated times and diluted 1:5 each step cross a chilled microtiter plate and pinned on growth media.

(E) Induced thermotolerance function of Hsp100 constructs in *E. coli*. ClpB deletion strains transformed with low copy plasmids expressing the indicated Hsp100 under the control of the ClpB promoter were grown at 30°C to mid-log, shifted to 42°C for 15 minutes and exposed to 50°C for the indicated times. Aliquots were removed and diluted 1:10 each step across a chilled microtiter plate and pinned on growth media.

In our initial assays of functionality, we tested the ability of our Hsp100 constructs to refold heat-denatured luciferase, a robust reaction of Hsp104 and ClpB that is known to rely upon Hsp70/40 co-chaperones. We replaced a centromeric plasmid expressing wildtype HSP104 in a $\Delta hsp104$ yeast strain with a series of plasmids expressing Hsp104, 444B, ClpB or BBB4 from the same native HSP104 promoter. Yeast expressing Hsp104 and 444B were able to rescue heat-denatured luciferase, while yeast expressing ClpB and BBB4 showed the same flat activity signal as the empty vector control (Fig 1c). Absolute luciferase reactivation by 444B was about 50% that of Hsp104. However, expression of 444B was consistently around 67% that of Hsp104 (Appendix A, Fig 1a), indicating the relative efficiency of 444B was significantly higher than the absolute value. In order to assay a wider range of substrates, we then tested the ability of our Hsp100s to convey induced thermotolerance in yeast. In agreement with our luciferase reactivation results, we found that 444B was able to rescue yeast transiently exposed to high temperatures at about 75% the level of Hsp104, while ClpB and BBB4 showed little effect over background (Fig 1d).

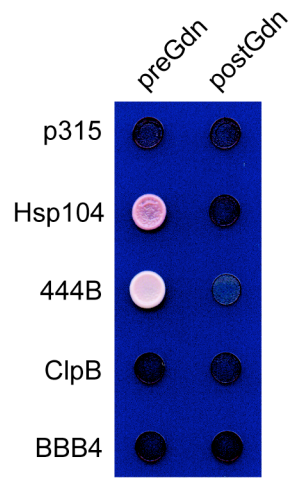
The failure of BBB4 to work in yeast could be due to inability to cooperate with host machinery or simply because it was catalytically dead. If the former were true, BBB4 but not 444B would function in bacteria just as 444B but not BBB4 functioned in yeast. We tested this assumption using induced thermotolerance in $\Delta clpB$ bacteria carrying low copy plasmids expressing our Hsp100s from the native *ClpB* promoter. We found that BBB4 did, in fact, enable bacteria to survive exposure to high temperatures at approximately the same level as ClpB, while neither Hsp104 nor 444B was able to show activity above the empty vector background despite being very well expressed (Fig 1e;

Appendix A, Fig 1b). Using yeast Hsp104/Pgk1 and bacterial Hsp104/RNAPbeta as internal normalization controls, we found that the ratio of 444B/BBB4 signal was 1.6 in yeast and 1.5 in bacteria. Therefore, failure of 444B in bacteria and of BBB4 in yeast cannot be attributed to expression level differences (Appendix A, Fig 1a and 1b). The results of our yeast and bacterial experiments together show the Hsp70/40-dependent thermotolerance activities of Hsp104 and ClpB reside in AAA1 and the accessory NTD and CC domains and strongly suggest that there is no necessary downstream physical coupling to the Hsp70/40 system for these activities.

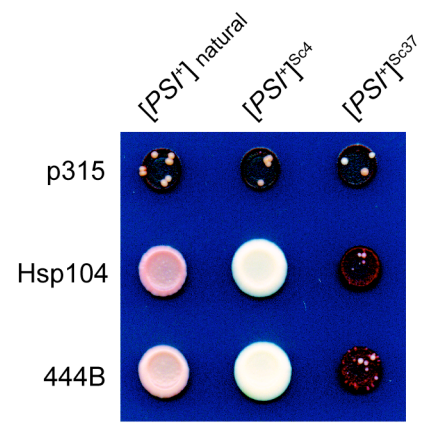
Prion inheritance is supported by 444B

We next tested whether our Hsp100s could support prion propagation by replacing native Hsp104 in $[PSI^+]$ yeast. In line with our findings for thermotolerance functions, the ability of our Hsp100s to support $[PSI^+]$ propagation was independent of the specific AAA2 present (Fig 2a). Neither ClpB nor BBB4 was able to maintain $[PSI^+]$, but 444B was able not only to maintain $[PSI^+]$ but tended to strengthen the aggregation-dependent nonsense suppression phenotype. The latter observation pointed to a possible variant preference in 444B activity. Yeast prions occur in variants based upon the physical conformation of the aggregate underlying the phenotype [19]. In order to test whether 444B could maintain multiple variants of $[PSI^+]$, we used the same plasmid shuffle assay using strains exhibiting defined $[PSI^+]$ variants, $[PSI^+]^{Sc4}$ and $[PSI^+]^{Sc37}$. As with the naturally-occurring $[PSI^+]$, 444B was able to support both defined variants (Fig 2b).

A



B



C

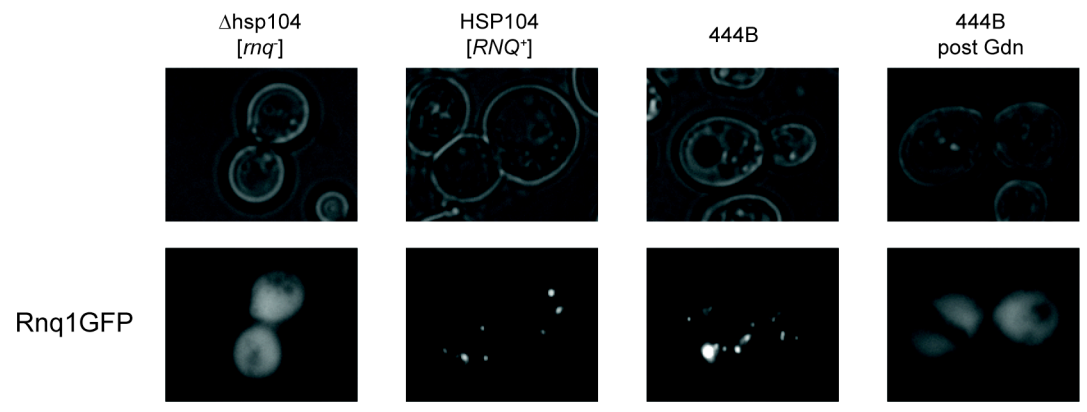


Figure 2. Prion propagation in yeast relies upon the endogenous top ring of Hsp104.

(A) [*PSI*⁺] HSP104 deletion strains carrying a URA-marked centromeric plasmid with Hsp104 under its native promoter were transformed with LEU-marked centromeric plasmids with the indicated Hsp100 under the control of the HSP104 promoter.

Transformants were plated on media selective for the LEU plasmids and counterselective for the original URA plasmids, and representative isolates were chosen for passage on 3mM GdnHCl. Pre- and post-curing isolates are shown on low adenine containing selective media. [*PSI*⁺] appears white to pink and [*psi*⁻] appears red and display impaired growth.

(B) Native Hsp104 on a URA-marked centromeric plasmid was replaced by an empty vector, by Hsp104 or by 444B as in (A) in yeast strains with the indicated [*PSI*⁺] variants. [*PSI*⁺] refers to a naturally-occurring variant, and [*PSI*⁺]^{Sc4} and [*PSI*⁺]^{Sc37} refer to variants created by infection of [*psi*⁻] yeast with recombinant Sup35 fibers polymerized at the indicated temperatures. Isolates are shown on low adenine containing selective media. Strong [*PSI*⁺] are white to pink, weak [*PSI*⁺] appear red and display an intermediate level of growth, and [*psi*⁻] appear red and display impaired growth.

(C) HSP104 was replaced in a [*PSI*⁺] [*RNQ*⁺] strain by 444B. [*RNQ*] status of the resulting 444B strain and its prion-cured derivative was assessed by a fluorescent assay in which [*RNQ*⁺] yeast display foci and [*rnq*⁻] yeast display diffuse fluorescence.

To establish the generality of prion maintenance function, we looked at the ability of 444B to sustain another yeast prion, $[RNQ^+]$. $[RNQ^+]$ is readily detected by the existence of fluorescent foci in cells expressing GFP fusions to the Rnq1 protein [33]. In order to assay $[RNQ^+]$ maintenance, we replaced the endogenous HSP104 locus with 444B in a natural $[PSI^+]$ $[RNQ^+]$ yeast strain. We found that 444B yeast maintained the ability to form Rnq1-GFP foci and that such foci disappeared after treatment with 5mM guanidine hydrochloride (Fig 2c). Our results demonstrate that neither thermotolerance nor prion propagation relies upon the AAA2 of the native Hsp100, with a major implication being that any downstream action of Hsp70/40 on substrates does not require a physical coupling to the exit of the translocation machinery.

444B can be adapted to couple to a substrate reporting “trap”.

Having demonstrated that only the top ring of Hsp104 was specifically needed for $[PSI^+]$ propagation, we sought to adapt our 444B chimera to monitor flux of prion substrates through the hexamer. Hsp104 family members include a group of Clp/Hsp100 proteins in bacteria that unfold tagged or aggregated proteins and feed them into the ClpP peptidase chamber for destruction. A proteolytically-inactive version of the peptidase, ClpP^{trap} (Trap) [47] was previously used to characterize the substrates of its natively docking Hsp100, ClpX. A subsequent study then exploited this trapping strategy to study the mechanism of ClpB, the only Clp that does not couple to the peptidase chamber, by engineering the ClpP-coupling “P element” of family member ClpA into ClpB, creating BAP [40]. Because BAP was altered only in AAA2, we could simply use the same design to create a ClpP-docking variant of 444B, which we called 4BAP (Fig 3a). We

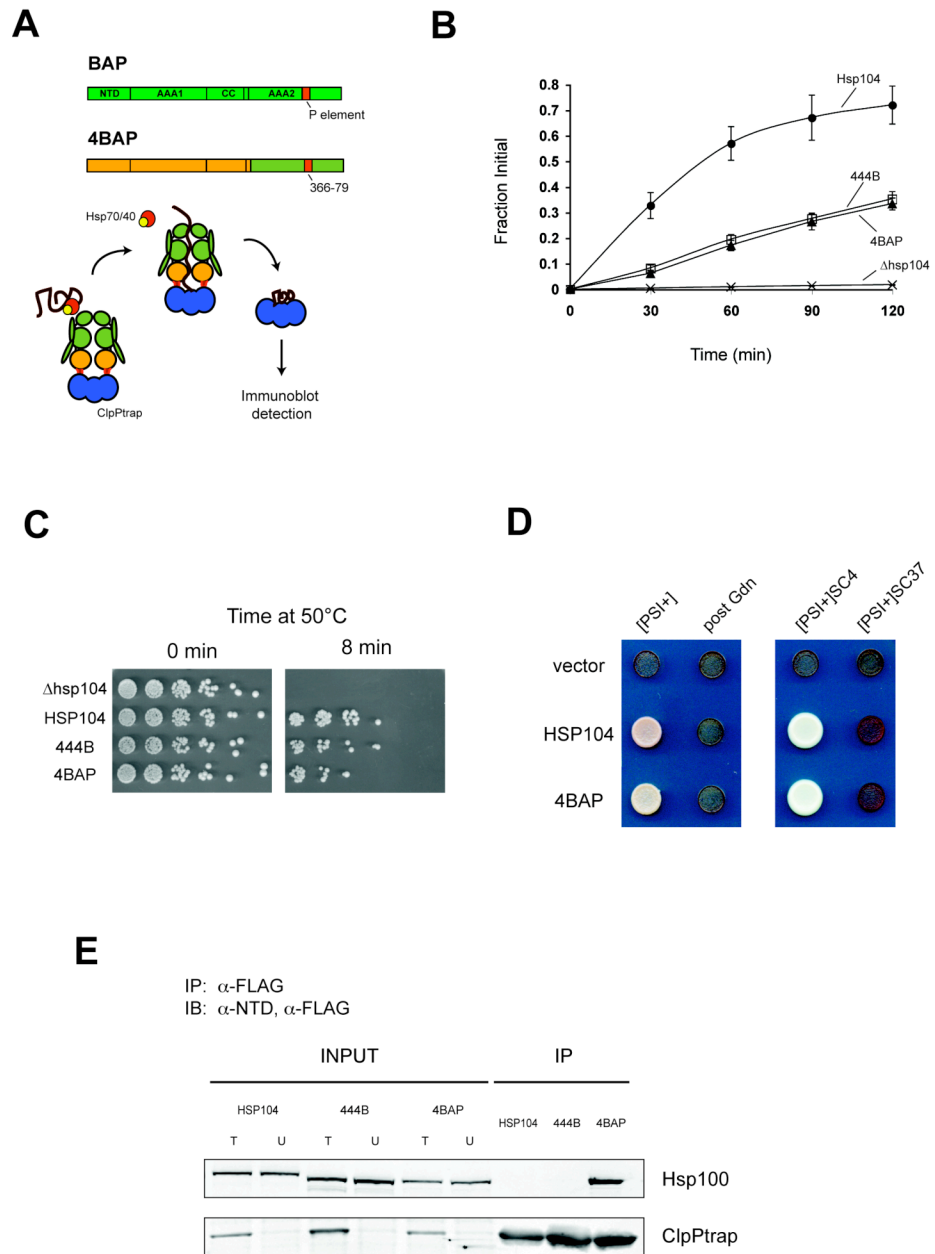


Figure 3. 444B can be altered to form 4BAP, a protease-coupling Hsp100.

(A) Schematic of 4BAP and its coupling to Trap.

(B) Luciferase reactivation by 4BAP, performed as in Fig 1c.

(C) Induced thermotolerance function by 4BAP, performed as in Fig 1d.

(D) Propagation by 4BAP of naturally-occurring [*PSI*⁺] and its curing by 5mM GdnHCl and propagation by 4BAP of defined [*PSI*⁺]^{Sc4} and [*PSI*⁺]^{Sc37} performed as in Fig 2b.

(E) Co-immunoprecipitation of 4BAP but not Hsp104 or 444B with TrapFLAG. Strains expressing TrapFLAG under the control of the strong constitutive TDH promoter and expressing the indicated Hsp100 integrated at the HSP104 locus were grown to early stationary phase. Anti-FLAG resin was incubated with cleared extracts, washed with low and high salt IP buffer and eluted with boiling SDS loading buffer. Total input (T), unbound extract (U) and 50X elution samples were separated by SDS-PAGE and probed with anti-Hsp104NTD and anti-FLAG.

tested the ability of 4BAP to reactivate heat-denatured luciferase (Fig 3b), convey thermotolerance (Fig 3c) and propagate all previously tested variants of [*PSI*⁺] and [*RNQ*⁺] (Fig 3d and data not shown) and found that 4BAP behaved in all assays essentially identically to 444B. We then expressed from the strong, constitutive TDH promoter an epitope-tagged Trap (TrapFLAG) in yeast carrying 444B, Hsp104 or 4BAP to check for specific coupling. We found that TrapFLAG (hereafter referred to as Trap) effectively coupled to 4BAP but not to 444B nor to Hsp104 (Fig 3e).

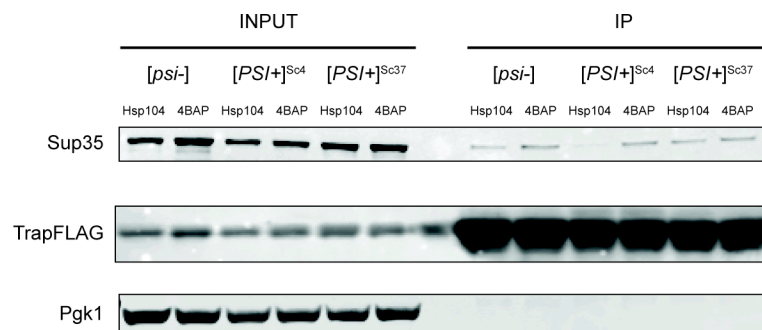
4BAP demonstrates translocation of aggregated amyloidogenic proteins

We exploited this coupling of 4BAP to Trap to investigate prion protein flux through the Hsp100 in cells both with and without prion aggregates. We saw anti-FLAG co-immunoprecipitation of Sup35 in both [*psi*⁻] and [*PSI*⁺] cells at a steady state high-level expression of Trap and a natural, Hsp104-promoter-driven level of 4BAP (Fig 4a). However, the signal (IP/input) in [*psi*⁻] cells was not dependent upon the presence of a docking (Trap-coupling) chaperone and could be attributed to nonspecific deposition on the beads of soluble Sup35 during the 3-5 hour binding reaction. This [*PSI*⁺]-specific translocation of Sup35 agrees with a recent study using a similar ClpP-docking version of Hsp104 (HAP) [48].

Coupling of 4BAP to Trap was unusually stable, as high salt washes failed to dislodge the chaperone from Trap. To address the possibility that Sup35 was binding to 4BAP alone, we performed the reciprocal experiment to the anti-FLAG immunoprecipitation. Using anti-NTD coupled to Protein A/G agarose, we immunoprecipitated 4BAP from 4BAP [*PSI*⁺], 4BAP-Trap [*psi*⁻] and 4BAP-Trap [*PSI*⁺]

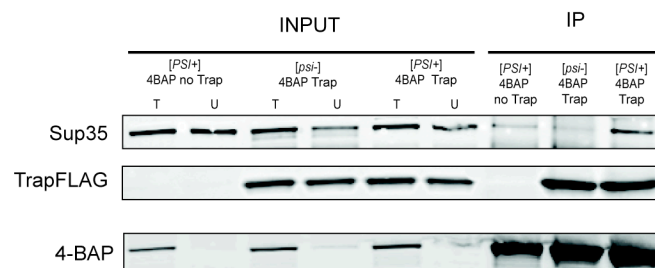
A

IP: α -FLAG
 IB1: α -SupNM, α -FLAG
 IB2: α -PGK1



B

IP: α -NTD
 IB1: α -SupNM, α -FLAG
 IB2: α -NTD



C

IP: α -FLAG
 IB1: α -Rnq1, α -FLAG
 IB2: α -PGK1

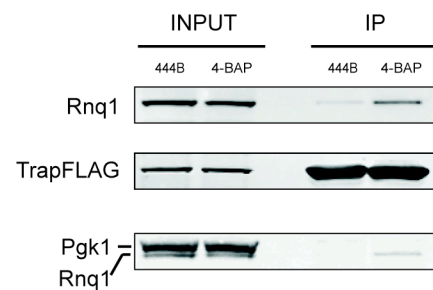


Figure 4. 4BAP translocates prion proteins in an aggregate-dependent fashion.

(A) Representative blot from the co-immunoprecipitation of Sup35 with TrapFLAG in [*psi*⁻], [*PSI*⁺]^{Sc4} and [*PSI*⁺]^{Sc37} 4BAP-Trap. Cleared yeast extracts were incubated with anti-FLAG resin. Resin was washed in low and high salt IP buffer and eluted with boiling SDS loading buffer. Input and 25X elution samples were separated by SDS-PAGE and probed with anti-SupNM, anti-FLAG and anti-Pgk1. Quantitation was conducted by using the LiCor Odyssey densitometry software and dividing IP values by INPUT values.

(B) Co-immunoprecipitation of Sup35 with 4BAP in [*PSI*⁺] strains expressing Trap. Cleared yeast extracts were incubated with Protein A/G agarose coupled to anti-Hsp104NTD antibodies. Agarose was washed in low and high salt IP buffer and eluted with boiling SDS loading buffer. Total input (T), unbound extract (U) and 50X elution samples were separated by SDS-PAGE and probed with anti-SupNM, anti-FLAG and anti-Hsp104NTD.

(C) Co-immunoprecipitation of Rnq1 with TrapFLAG in a [*RNQ*⁺] 4BAP-Trap strain. IP was performed as in (A) and blot was probed with anti-Rnq1, anti-FLAG and anti-Pgk1.

yeast. 4BAP was quantitatively immunoprecipitated from all yeast strains, but a clear Sup35 signal was seen only in a Trap-dependent, $[PSI^+]$ -dependent fashion (Fig 4b).

We extended the use of the 4BAP-Trap yeast system to explore action on different amyloid conformations. Significantly, Sup35 immunoprecipitated in 4BAP $[PSI^+]^{Sc4}$ cells (IP/input) was 3-fold higher than the background in HSP104 $[PSI^+]^{Sc4}$ and only around 20% higher than background in $[PSI^+]^{Sc37}$ (Fig 4a). This capture of Sup35 was specific to 4BAP recognition, as the abundant, soluble protein Pgk1 was not detected in any immunoprecipitated fractions (Fig 4a).

We next tested immunoprecipitation of Rnq1 in 4BAP-Trap $[rnq^-]$ and $[RNQ^+]$ yeast. As with Sup35 and $[PSI^+]$, anti-FLAG resin pulled down much more Rnq1 over deposition background in $[RNQ^+]$ (Fig 4c) than in $[rnq^-]$ cells (data not shown). The results in the different $[PSI^+]$ variants and in $[RNQ^+]$ suggest that 4BAP preferentially recognizes yeast prion proteins when they are in an aggregated form.

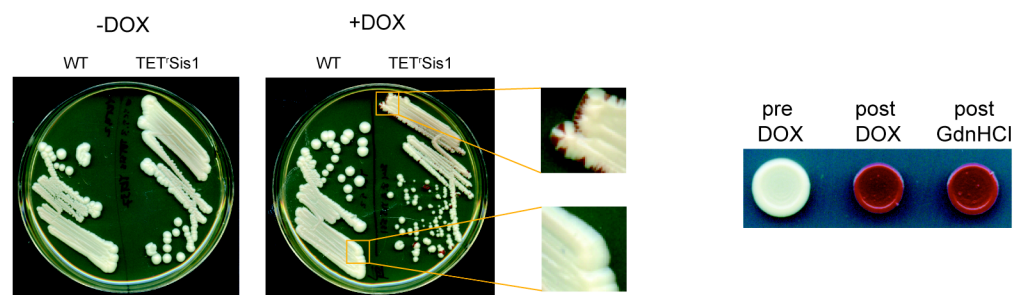
Suppression of the Hsp40 Sis1 abrogates translocation and prion propagation

Having shown prion-dependent translocation of Sup35 and Rnq1 through 4BAP, we next turned to the question of whether the Hsp70/40 system was acting upstream of the Hsp100. Previous work used a doxycycline-repressible allele of the Hsp40 Sis1 to show the involvement of Sis1 in $[RNQ^+]$ aggregate size and prion maintenance [33]. However, it was not clear from these experiments at what point in the propagation cycle Sis1 was acting. We obtained and mated this repressible Sis1 $[RNQ^+]$ yeast strain into our 4BAP $[PSI^+]^{Sc4}$ strain to generate Sis1-repressible $[PSI^+]$ HSP104 and 4BAP strains. Our initial test of Sis1 involvement in $[PSI^+]$ maintenance was growth of HSP104

TET^rSIS1 [*PSI*⁺]^{SC4} strains on doxycycline-containing media to assay for prion loss. We found that growth on doxycycline did, indeed, result in loss of [*PSI*⁺] as demonstrated by red sectoring (Fig 5a, left and enlargements) and that this was a permanent curing of [*PSI*⁺] as the red phenotype persisted when yeast were transferred to fresh media lacking doxycycline (Fig 5a, right). Our finding that [*PSI*⁺] was reliant upon Sis1 makes it clear for the first time that [*PSI*⁺] is not simply affected by but critically depends upon a chaperone other than Hsp104 for its maintenance.

We then turned to our 4BAP TET^rSIS1 strains to determine whether Sis1 was required for 4BAP translocation of prion proteins. For these experiments, we chose to use a Gal1-inducible TrapFLAG from a high-copy plasmid instead of our chromosomal TrapFLAG to enable us to control the timing of substrate trapping. We found that Sup35 was efficiently immunoprecipitated in [*PSI*⁺] strains in the absence of doxycycline but that levels decreased 12-fold relative to the input in the presence of the drug (Fig 5b, left), which resulted in an 80% decrease in Sis1 levels (Appendix A, Fig 2a). Again, the signal was specific as there was no detectable Pdk1 in the elution (Appendix A, Fig 2a). During the course of the Sis1 repression, [*PSI*⁺] was maintained, as platings of yeast treated with doxycycline at the time of harvest retained the nonsense suppression phenotype (Appendix A, Fig 2b). We tested for the same phenomenon in a [*RNQ*⁺] 4BAP TET^rSIS1 isolate and observed a 3-fold decrease in Rnq1 resulting from a 71% decrease in Sis1 (Fig 5b, right; Appendix A, Fig 2c). Taken together, our results strongly suggest the natural yeast prion propagation cycle is an Hsp70/40-dependent action of Hsp104, with Sis1 acting upstream of Hsp104 to recognize prion aggregates and recruiting Hsp104 for subsequent fragmentation and multiplication of amyloid aggregates.

A



B

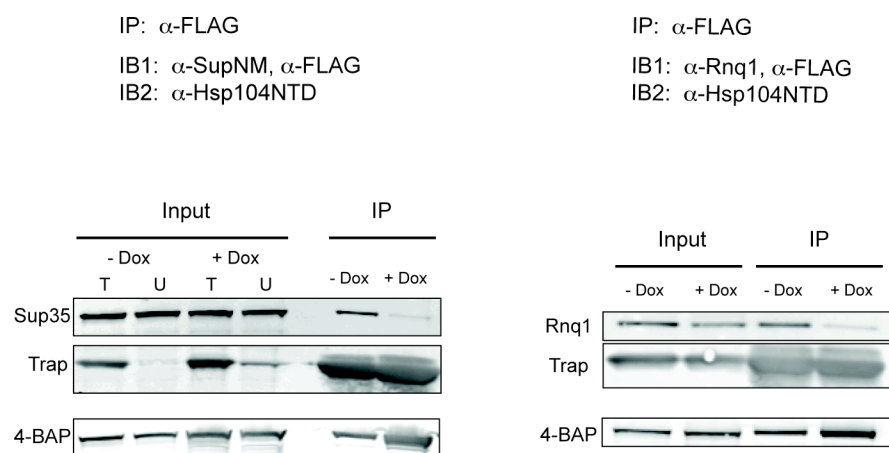


Figure 5. $[PSI^+]$ propagation and prion protein translocation depend upon the Hsp40 Sis1.

(A) $[PSI^+]$ was introduced into Δ sis1-[TETrSIS1] by mating and sporulation. SIS1 wild-type and Δ sis1-[TETrSIS1] sister spores were plated on rich media with or without doxycycline. Blowups of strains on doxycycline show red sectors indicative of $[PSI^+]$ loss in the TETrSIS1 but not in the SIS1 strain. Right: Δ sis1-[TETrSIS1] $[PSI^+]$ strains before and after passage on doxycycline or 5mM guanidine hydrochloride grown on rich media.

Discussion

We have developed a system for dissecting the pathway of yeast prion propagation *in vivo* and used this system to identify a new pathway component upstream of Hsp104. Our system allows us to bring increased clarity to studies that have been hampered *in vivo* by indirect, sometimes contradictory readouts and hampered *in vitro* by pleiotropic activities, some of which are unnecessary for the prion cycle *in vivo*.

In the course of constructing our *in vivo* prion-monitoring system, we established that the ClpB/Hsp104 architecture shows a surprising modularity of function and create two chimeras that will allow for a greater understanding of ClpB and Hsp104 function. The functional modularity of the ClpB/Hsp104 architecture might have been predicted by the evolutionarily distinctness of AAA1 and AAA2 [50]. That is, AAA1 of ClpB and Hsp104 are more closely related to each other than they are to the AAA2 within the same molecule, indicating a gene fusion event created these chaperones. Previous studies of domain contribution to catalysis and hexamerization assigning reversed roles of the rings of ClpB and Hsp104 [51, 52]. Biochemical studies of ClpB and Hsp104 have shown communications between the AAA1 and the AAA2 [51, 53] occur as a part of the catalytic cycle, communications that likely will be altered in our chimeras. Although we constructed 444B and BBB4 as tools for *in vivo* experiments, analysis of their biochemical properties and their cooperation with co-chaperones *in vitro* should clarify the shared mechanisms of the ClpB/Hsp104 family as well as how alterations in interdomain communication may affect the Hsp100 reaction cycle.

The inability of the yeast Hsp70/40 system to cooperate with ClpB along with the Hsp70/40-dependent refolding of luciferase and propagation of [*PSI*⁺] by 444B and

4BAP indicate there is no necessary downstream physical coupling of the 70/40 system or other chaperone systems to Hsp104 for these processes. Successful replacement of Hsp104 AAA2 also indicates the Hsp90 system, found to couple to Hsp104 through its C-terminus [54], plays no obligatory role in thermotolerance or prion propagation. Together, our data suggests a model of prion propagation illustrated in Figure 6. Sup35 aggregates (purple) are recognized by Ssa1/2 (red) and Sis1 (yellow) and recruited to the top ring of Hsp104 (gold). One or more Sup35 monomers are transferred to Hsp104, where translocation ensures separation of the engaged monomer from the fiber substrate and generates two new surfaces for fiber growth. The end of the translocation cycle results in the release of an unfolded Sup35 monomer, which may fold unassisted or with assistance from nearby chaperones, or add on to the end of a nearby fiber.

We now have in hand the tools to dissect the steps of prion propagation *in vivo* and the possibility of recreating an *in vitro* system that faithfully represents the true propagation cycle of $[PSI^+]$ and other yeast prions. It is clear now that the infective unit of $[PSI^+]$ is the amyloid fiber [19], but it is also clear that not all amyloids are prions. Adding oligopeptide repeats from Sup35 to a generic poly-Q stretch transforms an amyloid into a yeast prion [3] and scrambling the sequence of the prion domain of Sup35 results in many amyloids but fewer yeast prions [55, 56]. For any amyloid to be a yeast prion, its structure must be amenable to action of the cellular machinery. With these tools, we can now answer which structures are recognized and how well, and we can ask which structures can be efficiently acted on by the central Hsp100 machine. For

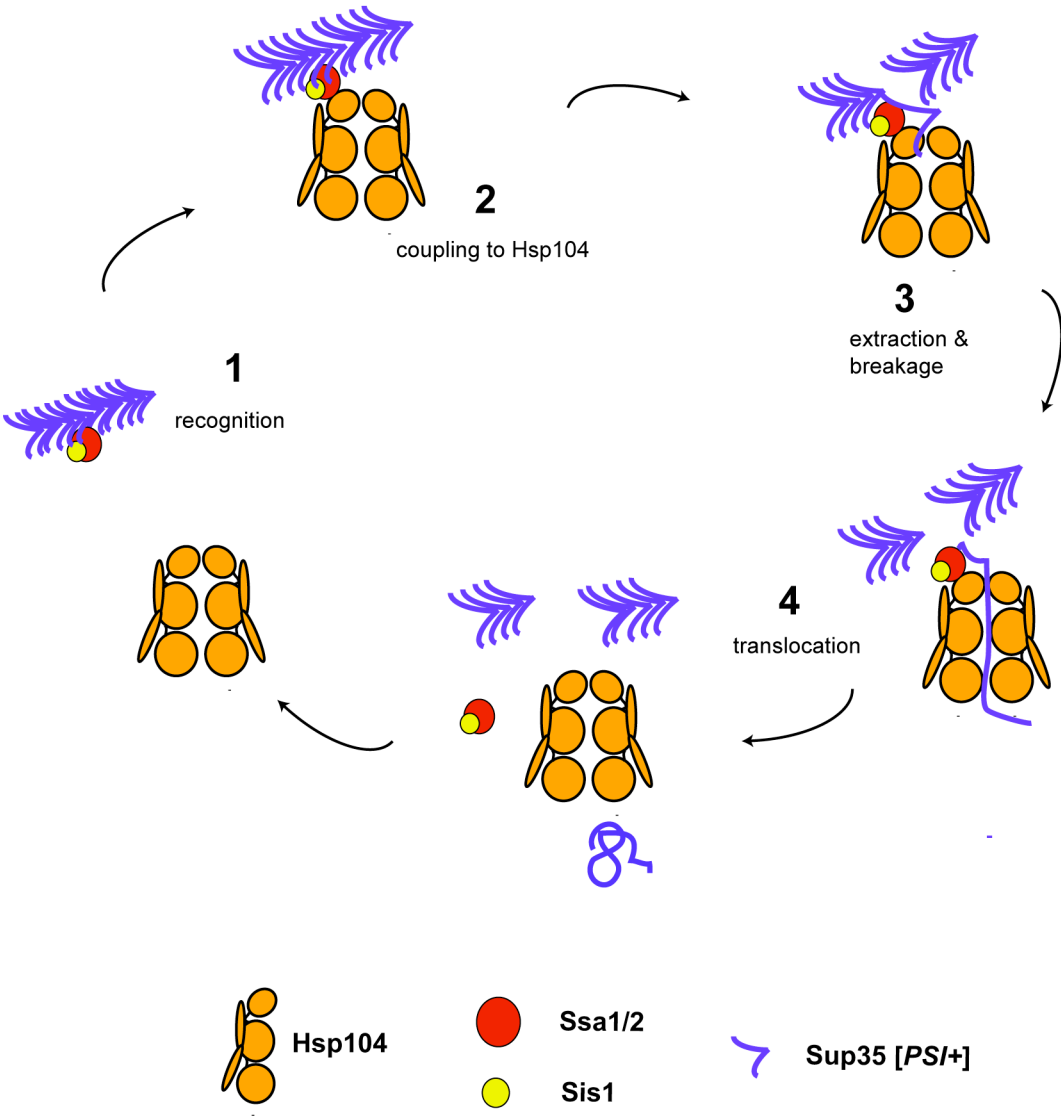


Figure 6. Model of Hsp104 cooperation with the Hsp70/40 system in propagating yeast prions.

Sup35 amyloid aggregates (purple arrowheads) are recognized by Sis1 (yellow) and Ssa1 (red) **(1)** and are recruited to Hsp104 **(2)**. A Sup35 subunit is transferred to Hsp104 at the pore entrance of the hexamer **(3)**, and the ATP-dependent translocation activity extracts the monomer from the fiber, generating two new ends for prion growth **(4)**.

example, $[PSI^+]^{Sc37}$ is composed of physically more rigid fibers than $[PSI^+]^{Sc4}$ and has fewer infective elements, or propagons, *in vivo*. The increase we consistently observed in the amount of Sup35 translocated in the strong $[PSI^+]^{Sc4}$ variant compared with the weak $[PSI^+]^{Sc37}$ variant agrees well with both the physical characterization of the fibers of $[PSI^+]^{Sc4}$ as more fragile [57] and the structural data indicating potential chaperone binding sites in Sc4 fibers are less protected than in Sc37 fibers [58]. The 4BAP-Trap system can be exploited to dissect the prion propagation reaction into discrete steps of initial recognition, transfer to 4BAP, engagement with the translocation machinery and translocation. Use of varying conformations will help define what sequence or structure Ssa1/Sis1 recognizes, which conformations are more readily transferred to Hsp104 and the effect of conformations on the unfolding and translocation steps.

Our studies demonstrate that prion propagation, like other aggregate remodeling reactions, critically depends upon recognition and recruitment to Hsp104 by co-chaperones. Hsp100 translocation machines have evolved accessory domains and coevolved with other cellular factors to restrict access to the unfolding activity of the central pore. It is perhaps not surprising that Hsp104 shows only weak interactions with its prion substrates, as the general pattern with these machines is that specificity is accomplished by collaboration with adaptors and co-chaperones. A strong recognition for one substrate would necessarily limit interactions with other substrates. We now have tools in hand for dissecting the individual steps of prion propagation *in vitro* with a system that faithfully recapitulates the natural cycle *in vivo*.

Materials and Methods

Strains and Plasmids

All yeast strains are derived from W303 strains YJW1070 (MATa *ura3::kan*) and YJW1068 (MATalpha *ura3::nat*): $[RNQ^+]$ $[PSI^+]$ *leu2-3,112 his3-11,15 trp1-1 ade1-14 can1-100*. Defined $[PSI^+]^{SC4}$ and $[PSI^+]^{SC37}$ strains were constructed from $[psi^-]$ $[rnq^-]$ strains (created by curing on 5mMGdnHCl) by protein infection as described previously [19] or by mating into such strains. HSP104 allele replacements were constructed by transforming wild-type or *hsp104::HIS3* yeast with DNA fragments containing the desired Hsp100 allele marked by TRP1 150bp into the 3'utr and selecting on Trp dropout media. Strains were confirmed by PCR and western blot. ClpP^{trap}FLAG (TrapFLAG) strains were constructed by replacing *ura3::NAT^r* with *ura3::kan_TDH1_TrapFLAG* in a similar fashion.

TET^rSis1 strains were constructed by mating into W303 *sis1-Δ*[TET^rSIS1], a gift of E. Craig and described previously [33].

Bacterial strains MC4100 wild-type and Δ *clpB::kan* were provided by B. Bukau and the *E. coli* Genetic Resource Center with the kind assistance and advice of D. Seigle.

Trap knockin templates were constructed (Katherine Verges) by amplifying ClpP without the 13-amino acid propeptide from DH5 α and cloning into pFA6a-kanMX6. ClpP S97A (Trap) [47] was constructed by QuikChange (Stratagene). Standard cloning techniques were used to insert the TDH3 and GAL1 promoters, the 3xFLAG epitope tag and to subclone the GAL1_TrapFLAG cassette into p426.

The HSP104 coding region, promoter and 3'utr were amplified from *S. cerevisiae* genomic DNA, and the ClpB coding region, promoter and 3'utr were amplified from DH5 α *E. coli*. A modular system of promoter-coding-3'utr was created in p315 for yeast and pSU18 for bacteria for ease of gene replacement. All chimeras were constructed by fusion PCR using cloned HSP104 and ClpB as templates, and all constructs were confirmed by sequencing.

Yeast prion propagation

[*PSI*⁺] propagation was determined by plasmid shuffle assay replacing pKAT136 (pRS316 HSP104) in YKT12, 24 or 26 with pRS315 HSP104, ClpB, 444B, BBB4 or 4-BAP under the control of the HSP104 promoter as follows: the parent strain was grown in synthetic media lacking uracil overnight, backdiluted in rich media to allow loss of pKAT136, transformed with the appropriate plasmids and plated on synthetic media lacking leucine and supplemented with 5-fluorouracil. [PSI] status was determined by color phenotype on low Adenine media and growth on trace Adenine or no Adenine media.

[*RNQ*⁺] propagation was determined by foci formation in strains transformed with 416CUP1pRNQ-GFP (gift of E. Craig) after 4 hours of induction with 50 μ M CuSO₄, or by [*psi*⁻] to [*PSI*⁺] conversion by 50 μ M CuSO₄ induction of 426CUP1pSupNM.

Thermotolerance Assays:

Induced thermotolerance assays in *S. cerevisiae* were performed essentially as described [59]. YKT52 (*hsp104::CgHIS3*) transformed with LEU2 CEN-ARS plasmids carrying

the indicated chaperone under the *HSP104* promoter were grown in synthetic media lacking leucine at 30°C to mid-log and shifted to 37°C for 30min. 1mL aliquots of the heat-treated cultures were added to prewarmed tubes in a 50°C water bath. Cells were taken at the indicated time points, serially diluted 5-fold each step in chilled microtiter plates, pinned on synthetic media lacking leucine and incubated 48-72 hours at 30°C.

Induced thermotolerance assays in *E. coli* were performed as described [40]. MC4100 and $\Delta clpB::kan$ transformed with pSU18 carrying the indicated chaperone under the *ClpB* promoter were grown in LB + 34µg/mL chloramphenicol at 30°C to mid-log, shifted to 42°C for 15 minutes, and 1mL aliquots were added to prewarmed tubes in a 50°C water bath. Cells were removed at the indicated time points and serially diluted (10-fold each step) in chilled microtiter plates, pinned on LB+chloramphenicol media and incubated 24 hours at 30°C.

Expression levels of chaperones in both *S. cerevisiae* and *E. coli* were confirmed by SDS-PAGE of soluble lysates followed by coomassie staining and/or immunoblotting with anti-ClpB and anti-Hsp104NTD antibodies normalized to an internal soluble standard, anti-Pgk1 (Invitrogen) for yeast and anti-RNAPbeta (Neoclone) for bacteria. Anti-ClpB and anti-Hsp104 antibodies were a gift of B. Bukau. Expression levels of untagged versions of our Hsp100s were assessed by using a mixture of Hsp104NTD-reactive and ClpB-reactive antibodies normalized against internal controls in yeast and in bacteria with Hsp104 levels in yeast being our reference point (Supplemental Figure 1).

Luciferase Refolding:

In *S. cerevisiae*, YKT52 (*hs104::CgHIS3*) derived strains transformed with p316GPDlux (gift of B. Bukau) and p315 carrying the indicated chaperone were grown to mid-log at 30°C, shifted to 37°C for 60min, heat shocked at 44°C for 60min with 20µg/mL cycloheximide added at 50min and shifted back to 30°C for 120min. Luciferase activity was measured before heat shock and at the indicated time points by adding 50µL 1mM Beetle Luciferin (Promega) to 100µL cells and taking 10second integrated luminescence signal in an EG&G Berthold MicrolumatPlus luminometer.

Immunoprecipitations:

For the prion capture experiments in uninduced conditions, cells were grown in YEPD to early stationary phase, OD₆₀₀ ~ 2.0 and harvested. For Sup35 induction experiments, cells were grown overnight in synthetic media lacking uracil (SD-Ura), backdiluted to OD₆₀₀ = 0.15 in SD-Ura supplemented with 10uM CuSO₄ and harvested at OD ~ 1-2. For Sis1 shutoff experiments, cells were grown in SD-Ura overnight, backdiluted to OD₆₀₀ = 0.15 in 2% raffinose-containing media (SR-Ura) and grown to OD₆₀₀ ~ 0.4. Cultures were supplemented with 2% galactose to induce TrapFLAG, split and half were treated with 5ug/mL Doxycycline. Cells were harvested at OD ~ 1.

For all immunoprecipitations, cells were lysed by vortexing with glass beads at 4C in IP buffer (50mM HEPES-KOH, pH 7.0, 150mM KOAc, 2mM MgOAc, 1mM CaCl₂, 0.1% Triton X-100) + Roche Complete Protease Inhibitor Cocktail, pepstatin A, 4mM EDTA and RNaseA. Whole cell lysates were cleared by centrifugation at 20,000g for 10min at 4C and the supernatants were bound at 4C to pre-equilibrated anti-FLAG beads (Sigma #F2426). Beads were washed at 4C with 3x IP buffer, 1x IP buffer + 1M

NaCl, 2x IP buffer and were eluted with either 3xFLAG peptide (Sigma) or with boiling 2x SDS-PAGE loading buffer.

Western Blots

Immunoblotting was performed according to standard procedures, using rabbit antisera specific for Sup35NM, for Hsp104 NTD (aa1-146), for full-length Hsp104 or ClpB (gifts of B. Bukau) or for Hsp104 C-terminal 15aa (Stressgen) and mouse monoclonal anti-FLAG (Sigma), mouse anti-Pgk1 (Molecular Probes), mouse anti-RNAP beta (*E. coli*) or mouse anti-Luciferase (EMD Biosciences) as primary antibodies and with AlexaFluor680- (Invitrogen) or IRDye800- (Rockland) conjugated goat anti-mouse and anti-rabbit antibodies as secondary antibodies. Blot signals were detected and quantitated using the LiCor Odyssey infrared imaging system and software.

Sc Strain	Description	Source
[PSI+]alpha	W303 <i>MATalpha leu2-3,112 his3-11,15 trp1-1 ade1-14 can1-100 ura3::nat</i> [RNQ+] [PSI+]	this study
[PSI+]a	W303 <i>MATa leu2-3,112 his3-11,15 trp1-1 ade1-14 can1-100 ura3::kan</i> [RNQ+] [PSI+]	this study
TETrSis1	W303 <i>MATalpha trp1-1 ura3-1 leu2-3,112 his3-11,15 ade2-1 can1-100 GAL2+ met2-Δ1 lys2-Δ2 Δsis1::LEU2-[TETrSIS1]</i> [RNQ+] [psi-]	E. Craig
YKT12	<i>hsp104::HIS3/p316hsHsp104</i> [PSI+] ^{Sc4}	this study
YKT24	<i>hsp104::HIS3/p316hsHsp104</i> [PSI+] ^{Sc37}	this study
YKT29	<i>hsp104::HIS3/p316hsHsp104</i> [PSI+]	this study
YKT44	<i>hsp104::4BAP-TRP1, sis1Δ-[TETrSIS1]</i> , [PSI+] ^{Sc4} [RNQ+]	this study
YKT50	<i>hsp104::444B-TRP1</i>	this study
YKT52	<i>hsp104::HIS3</i>	this study
YKT69	<i>hsp104::4BAP-TRP1</i> [psi-]	this study
YKT92	<i>hsp104::4BAP-TRP1</i> , [PSI+] ^{Sc4}	this study
YKT96	<i>hsp104::4BAP-TRP1</i> , [PSI+] ^{Sc37}	this study
YKT99	<i>ura3::TDHClpPTrapFLAG</i> , [psi-] [rnq-]	this study
YKT102	<i>ura3:: TDHClpPTrapFLAG</i> , [PSI+] ^{Sc37} [rnq-]	this study
YKT111	<i>hsp104::4BAP-TRP1, sis1Δ-[TETrSIS1]</i> , [PSI+] ^{Sc4} [rnq-]	this study
YKT141	<i>hsp104::4BAP-TRP1; ura3::TDHClpPTrapFLAG</i> , [psi-] [rnq-]	this study
YKT143	<i>ura3:: TDHClpPTrapFLAG</i> , [PSI+] ^{Sc4} [rnq-]	this study
YKT147	<i>hsp104::4BAP-TRP1; ura3::TDHClpPTrapFLAG</i> , [PSI+] ^{Sc4} [rnq-]	this study
YKT149	<i>hsp104::4BAP-TRP1; ura3::TDHClpPTrapFLAG</i> , [PSI+] ^{Sc37} [rnq-]	this study
E. coli Strain	Description	Source
MC4100 (CGSC #6152) <i>ΔclpB</i>	[<i>araD139</i>], (<i>ΔargF-lac</i>)169, <i>λ-</i> ; <i>e14-</i> , <i>flhD5301</i> , <i>Δ(fruK-yeiR)725(fruA25)</i> , <i>relA1</i> , <i>rpsL150(strR)</i> , <i>rbsR22</i> , <i>Δ(fimB-fimE)632(::IS1)</i> , <i>deoC1</i> [<i>araD139</i>], (<i>ΔargF-lac</i>)169, <i>λ-</i> ; <i>e14-</i> , <i>flhD5301</i> , <i>Δ(fruK-yeiR)725(fruA25)</i> , <i>relA1</i> , <i>rpsL150(strR)</i> , <i>rbsR22</i> , <i>Δ(fimB-fimE)632(::IS1)</i> , <i>deoC1</i> , <i>ΔclpB::Kan</i>	B. Bukau, <i>E.coli</i> GRC B. Bukau, <i>E.coli</i> GRC
Plasmid	Description	Source
pKAT112	pRS315_4hs_HSP104 (4hs = 500bp upstream of <i>HSP104</i>)	this study
pKAT116	pRS315_4hs_ClpB	this study
pKAT117	pRS315_4hs_444B	this study
pKAT118	pRS315_4hs_4BAP	this study
pKAT136	pRS316_4h_HSP104	this study
pKAT161	pRS315_4hs_BBB4	this study
pKAT172	pSU18_Bhs_ClpB (Bhs = 500bp upstream of <i>ClpB</i>)	this study
pKAT173	pSU18_Bhs_444B	this study
pKAT174	pSU18_Bhs_Hsp104	this study
pKAT175	pSU18_Bhs_BBB4	this study
pKAT184	p426_GAL1p_ClpPTrapFLAG	this study
pGPDlux	p316_GPD_luciferase (firefly)	B. Bukau
pRnq-GFP	p316_CUP_RNQ1msGFP	E. Craig
	Ura3-G418r-TDH3 or GAL1-ClpP or ClpPTrap 3xFLAG-cyc1-ura pFA6a-Kan-MX6; p416MET25	this study

Chapter 3

The N-terminal domain of Hsp104 alters prion variants in yeast

Introduction

The yeast prion $[PSI^+]$ relies upon a particular level of the chaperone Hsp104 for its stable maintenance in yeast [4]. Deletion or chemical inhibition of Hsp104 causes the loss of $[PSI^+]$ in dividing cells, and ectopic overexpression of Hsp104 causes the loss of $[PSI^+]$ [4]. Because prion infective units have been shown to be amyloid fibers [18, 19], this maintenance has been suggested to be a balance of prion amplification by fiber fragmentation [5, 7, 20] and prion dissolution by monomer resolubilization [6]. How this balance of amplification and dissolution is achieved is unclear. The fission yeast homolog of Hsp104, *Schizosaccharomyces pombe* Hsp104 (*Sp104*) is able to maintain $[PSI^+]$ in the absence of Hsp104 but is unable to cure $[PSI^+]$ when ectopically overexpressed (Peter Chien, personal communication and Fig 1a). In this study, I identified the N-terminal domain of Hsp104 (NTD) as necessary for the curing of $[PSI^+]$ by ectopic overexpression of Hsp104 and found that it alters prion variant phenotypes but not the underlying conformation of the amyloid. Further, I conducted random and targeted mutagenesis of the NTD that identified a surface patch containing two solvent-exposed loops important for these effects. These results reveal an important regulatory role of the Hsp104 NTD in substrate selection and in modulating the efficiency of substrate processing.

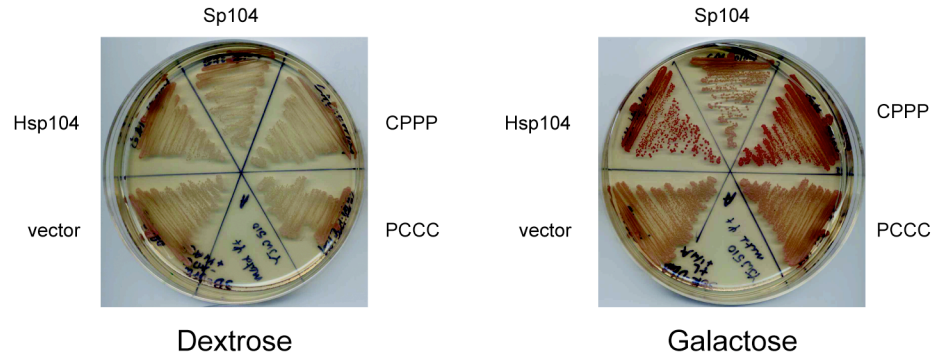
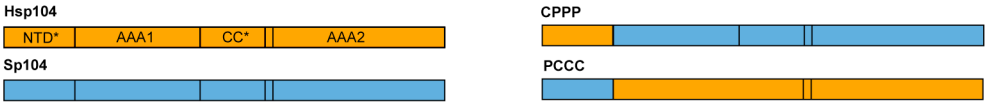
For the initial phase of this project, I continued a line of experiments started by Peter Chien during his graduate tenure in the Weissman lab. These experiments used a chimera-construction approach to identify the domain of Hsp104 responsible for the curing of $[PSI^+]$ by overexpression. Peter had determined that *Sp104* could propagate $[PSI^+]$ but could not cure $[PSI^+]$ when overexpressed. *S. pombe*, unlike budding yeast,

harbors few Q/N rich protein sequences and in particular has lost the prion-forming domain of Sup35 [60]. Peter reasoned that domains of *Sp104* may have diverged concomitantly with the loss of prion-forming abilities of Sup35. The Hsp100 family is characterized by central ATP-binding domains (AAAs) that mediate hexamer formation and hydrolyze ATP to generate the force necessary to thread substrates through the resulting central pore. Diversity and substrate specificity are achieved by expanding on the core hexamer with additional domains [9]. In the case of Hsp104, an N-terminal domain (NTD) and a coiled-coil (CC) domain (Fig 1a). My nomenclature for chimeras is to use C (*cerevisiae*) for Hsp104 domains and P (*pombe*) for *Sp104* domains, assigning a letter to each of the domains NTD-AAA1-CC-AAA2, such that Hsp104 would be CCCC and *Sp104* would be PPPP. Working with Peter, we selected the CC domain as the likely culprit and constructed two chimeras, PPCP (Hsp104 CC in the context of *Sp104*) and CCPC (*Sp104* CC in the context of Hsp104), and I tested their abilities to maintain and cure [*PSI*⁺]. To our surprise, CCPC but not PPCP was able to cure [*PSI*⁺] upon ectopic overexpression, and both chimeras were functional in prion maintenance (data not shown). At this point, the project was wholly turned over to me.

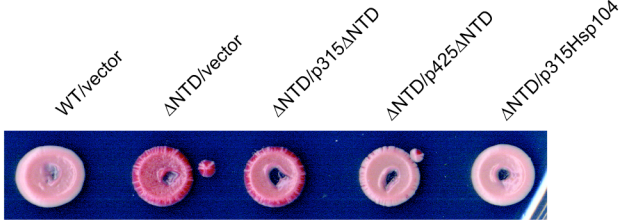
Results

My studies began by examining the role in [*PSI*⁺] maintenance of the NTD of Hsp104. Full-length Hsp104 and *Sp104* share 49% identity, 68% similarity, their CC domains share 42% identity, 61% similarity, while their NTDs share a lower 34% identity, 54% similarity, making the NTD an attractive target for functional differences. Initially, I constructed and tested chimeras CPPP and PCCC (Fig 1a). I introduced into a

A



B



C

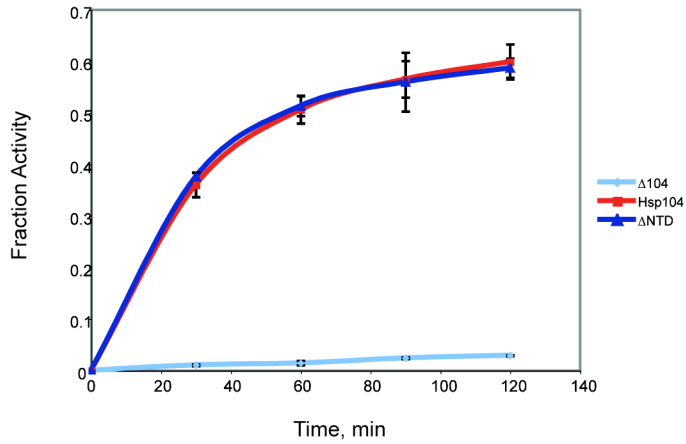


Figure 1. NTD of *S. cerevisiae* conveys prion-specific phenotypes. (A) The indicated Hsp100s under the control of the inducible GAL1 promoter were introduced into [PSI⁺] yeast. Transformants were streaked on dextrose (right) and galactose (left). Darkening color indicates solubilization of Sup35 and curing of [PSI⁺]. (B) Yeast with a chromosomal integration of Δ NTD and carrying the indicated Hsp104 allele under the native HSP104 promoter are compared to wild-type HSP104 [PSI⁺] yeast. Increasing dosage of Δ NTD reduces sectoring against a pale (strong variant) background while a single copy of Hsp104 reverts the [PSI⁺] state to wild-type. (C) Yeast carrying the indicated Hsp104 allele under the native HSP104 promoter and luciferase under the control of the constitutive GPD promoter were grown to mid-log at 30°C, shifted to 37°C for 1 hour, exposed to 42°C for 1 hour and allowed to recover after addition of cycloheximide at 30°C. Luciferase activity was measured at the indicated times and plotted as a fraction of the pre-42°C level for each culture.

[*PSI*⁺] yeast plasmids expressing from the GAL1 promoter Hsp104, *Sp*104, CPPP or PCCC along with an empty vector control. On dextrose media suppressing the Hsp100s, yeast were uniformly white. On galactose media expressing the Hsp100s at a high level, yeast carrying Hsp104 and CPPP showed the darker pigmentation indicative of [*PSI*⁺] curing (Fig 1a).

The isolation of the NTD of Hsp104 as responsible for overexpression curing of [*PSI*⁺] was interesting particularly in light of studies indicating the NTD of the bacterial homolog of Hsp104, ClpB, was dispensable for function [51, 61] but nonetheless bound aggregates [13, 62] and enhanced chaperone function [63]. To determine whether the Hsp104 N-terminal domain was equally dispensable, I constructed an allele of Hsp104 with amino acids 2-146 deleted (Δ NTD). Various plasmid shuffle assays showed Δ NTD was defective in stable prion maintenance (data not shown), and a chromosomal integration of Δ NTD showed heavy sectoring against a pale background (Fig 1b), indicating rapid prion loss in the context of a strong [*PSI*⁺] variant.

An inherent problem of the effect of Hsp104 dosage on [*PSI*⁺] is inhibition seems to phenocopy excess in that deletion and overexpression both result in [*psi*⁻]. However, extra copies of HSP104 result in a uniform darkening of color within individual colonies along with infrequent sectoring, while the Δ NTD phenotype resulted in sectoring against a pale, strong variant, background. To test the effect of dosage on the Δ NTD phenotype, I introduced centromeric and 2-micron plasmids encoding Δ NTD under the HSP104 promoter as well as a centromeric plasmid encoding Hsp104 into Δ NTD yeast. Instead of seeing a progressive darkening of background color, I observed a paler background color and a decrease but not an elimination in sectoring as the copy number of Δ NTD was

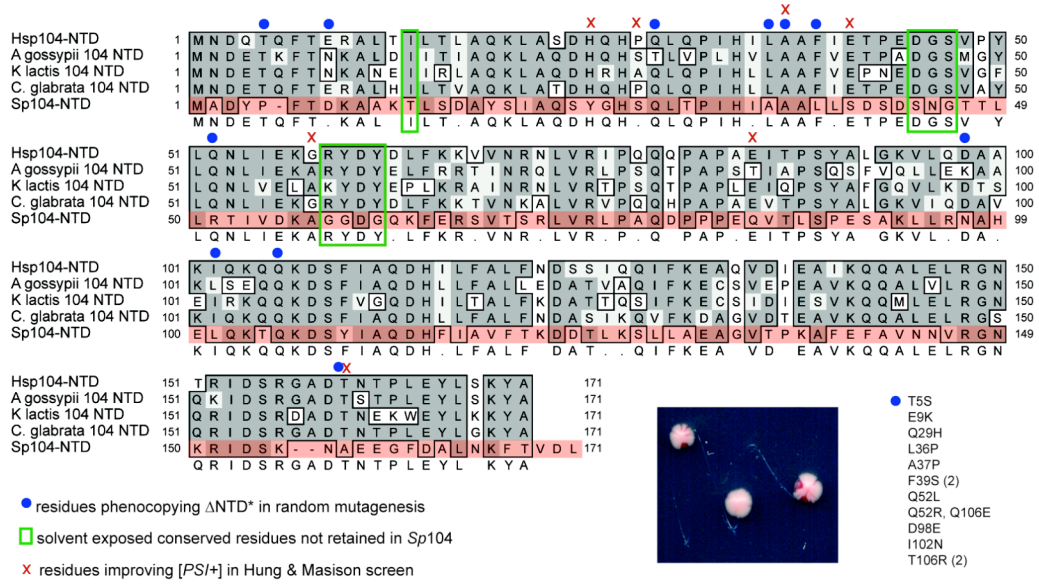
increased (Fig 2b). However, single centromeric plasmid encoding Hsp104 completely eliminated Δ NTD sectoring. In agreement with the results obtained in my chimera experiments, these results indicate that the sectoring phenotype of Δ NTD is a loss of function akin to inhibition of Hsp104 rather than a gain of function akin to Hsp104 overexpression.

To examine whether the Hsp104 NTD was able to support reactivation of heat-denatured aggregates, I compared the ability of Hsp104 and Δ NTD to refold luciferase expressed from a strong, constitutive promoter after denaturation at 42°C. As is the case in some ClpB studies [61], the NTD was dispensable for reactivating luciferase (Fig 1c) and was also not necessary for Hsp104-dependent survival during transient exposure to 50°C (data not shown). Therefore, the NTD of Hsp104 has a specific role in the efficient maintenance of prions.

In order to identify particular mutants responsible for the prion-destabilizing effect of Δ NTD (pictured in the inset at the bottom right of Fig 2a), I conducted dual mutagenesis screens: a random mutagenesis of the NTD in collaboration with my then rotation student Erin Quan and a targeted mutagenesis in conjunction with a crystallographic effort by my fellow graduate student Clement Chu.

Screening by random mutagenesis tended to hit residues (blue dots on Fig 2a) conserved in all yeast Hsp104s, including *Sp104*, and later mapping of these residues onto Clement's preliminary crystal structure revealed that many of these were likely domain-destabilizing mutants such alpha helix 2-breaking A37P. Of the surface-exposed residues, only Q25L was located in a promising location on the crystal structure model (discussed below).

A



B

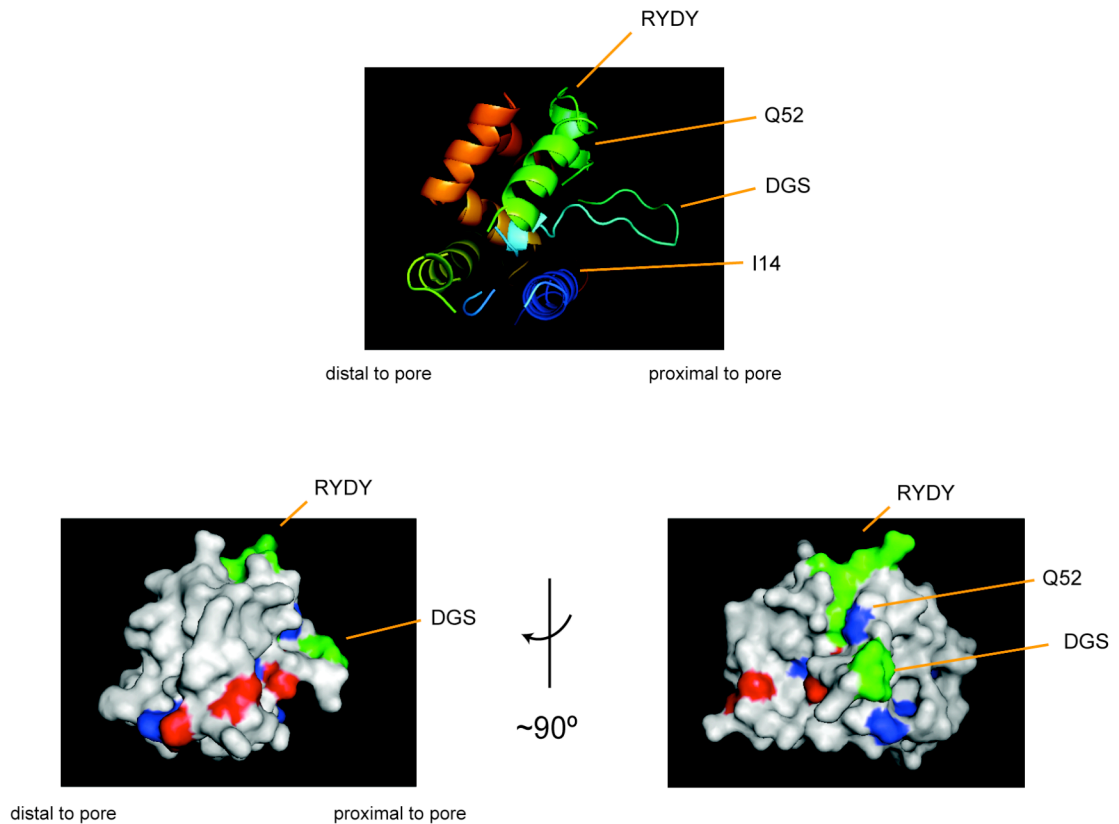


Figure 2. Random and targeted mutagenesis uncovers adjacent loops on the NTD crystal structure important for [PSI+] modulation. (A) CLUSTAL-W alignments of Hsp104 NTD with three other budding yeast homologs and the fission yeast *Sp*104 NTD (highlighted in orange). Green boxes highlight divergences in fission yeast, blue dots mark residues mutated in random screen which are listed at the bottom right, and red X's mark residues mutated in a random screen for mutants improving [PSI+] propagation[64]. Yeast in lower right panel show phenotype screened for in random mutagenesis and tested in targeted mutagenesis. (B) Top: ribbon representation of the preliminary Hsp104 NTD structure (Clement Chu) with helices colored in progression from the N-terminal dark blue. Labeled are the targeted loops and residue I14 and the random mutagenesis hit Q52. Bottom left: surface representation of the ribbon image from the same perspective. Residues are color coded as in (A). Bottom right: 90° rotation of surface representation to demonstrate the clustering of the residues affecting [PSI+]. This side of the NTD is proximal to the hexamer's pore [49], although the exact orientation is not clear.

Concurrent with my screens (in W303 wild-type yeast), the laboratory of Daniel Masison conducted a hydroxylamine (G:C to A:T transitions) mutagenesis of Hsp104 and screened for mutants that improved [*PSI*⁺] propagation in the yeast strain 779-6A in the background of a dominant Hsp70 mutant, SSA1-21, that destabilized [*PSI*⁺] [64]. My mutagenesis specifically targeted the NTD and used an enzyme combination that gave a wider array of possible mutations (G:C to A:T being ~25% of total changes; see Materials and Methods). The Masison lab uncovered several double mutations mapping throughout Hsp104 and several single mutations mapping to the NTD (red x's in Fig 2a), which when retested along with a Δ NTD construct (Δ 2-147) virtually identical to mine (Δ 2-146), in a wild-type SSA1 background, increased the strength of their [*PSI*⁺] variant. The destabilization that I observed was not reported by the Masison lab, but we were in agreement that loss of Hsp104 NTD led to failure to cure [*PSI*⁺] upon overexpression and had no effect on thermotolerance functions. Examination of the placement of the Masison mutations on Clement's crystal structure resulted in a similar pattern to my randomly-derived mutants. Many were likely to disrupt the NTD fold.

The Hung and Masison screen and the differing phenotypes I observed compared to this study deserve a bit of explanation. I asked for and received the strains used in the Masison screen and confirmed that their Δ NTD propagated a stable, stronger variant than did their wild-type Hsp104. Notably, the wild-type [*PSI*⁺] variant they used as a starting strain in their plasmid shuffle assays was a weaker, more unstable (sectoring) variant than the one I used in my studies. Further examination revealed that the Masison Hsp100s were expressed at 1.6-1.7 times the level of chromosomal Hsp104 and my Hsp100s were expressed at 0.6-0.7 times the chromosomal levels (data not shown and Fig 3a table).

Therefore, in the same allele replacement experiments, Hung and Masison started with a weak, unstable variant that was strengthened by replacement with Δ NTD while I started with a strong, stable variant that was destabilized but also strengthened in background color by replacement with Δ NTD. I believe that both phenomena are due to a loss of function exhibited by Δ NTD explained in more detail below. These differences emphasize the need for careful assessment of Hsp104 allele levels when interpreting effects on [*PSI*⁺].

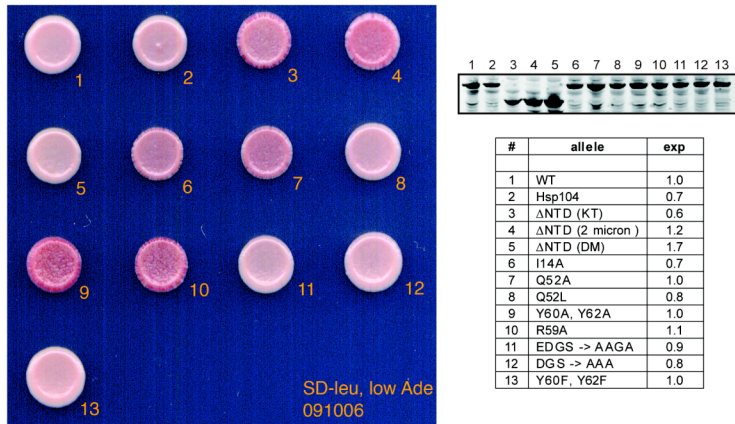
My analysis of the random mutagenesis candidates was greatly aided by the structural studies performed by Clement. As I finished sequencing my candidates and began to get duplicates, Clement successfully crystallized Hsp104 NTD (amino acids 1-158), obtained diffraction to 1.8 angstroms and quickly generated a preliminary version of the structure, which was very similar to the 8-alpha helix, 2-fold pseudo-symmetric ClpB NTD structure [65]. At this point, having reached the point of retaining redundant mutants, none of which were surface-exposed residues differing in *Sp*104 but conserved in budding yeast Hsp104s, and obtaining only Q52L that mapped to a promising surface change, I shifted to a more directed mutagenesis.

Alignment of the NTDs of budding and fission yeast revealed several residues and peptide stretches conserved in the prion-domain-harboring budding yeast that were lost in prion-domain-lacking fission yeast (green boxes in Fig 2a). Examination of the preliminary crystal structure of Hsp104 NTD showed that two stretches, DGS (residues 45-47) and RYDY (residues 59-62) were located in extended loops between alpha helices 2-3 (DGS) and 3-4 (RYDY) and that a conserved isoleucine (I14) was located adjacent to the DGS loop (Fig 2b, top). Interestingly, residue Q52, which was identified in the

random mutagenesis screen for [*PSI*⁺]-destabilizing NTD mutants, mapped to a surface between the RYDY and DGS loops (Fig 2b, bottom right). Although the NTD in the TClpB crystal structure [49] was found in three orientations 120° in rotational space with respect to the remainder of the protomer, it can still safely be said that this extended patch on the Hsp104 NTD is proximal to the hexamer pore, either lining the entrance or interfacing with adjacent NTDs.

To assess the relative functional contributions to of residues comprising this surface patch on the Hsp104 NTD as well as to directly compare them with the Δ NTD phenotype of the Masison screen, I replaced a native centromeric Hsp104 plasmid with a series of NTD mutants (see table in Fig 3a) and assessed their expression levels and phenotypes in comparison with a native chromosomal Hsp104 (Fig 3a). Strains were frogged on low adenine media to reveal the strength of the [*PSI*⁺] variant. Western blot levels of these strains are shown to the left above the table listing the mutants along with the quantitation of Hsp104 expression normalized to the internal control P_{gk1} and to wild-type (#1). Examination of the phenotypes reveals that at the same or greater expression relative to Hsp104 (#2), Δ NTD (#3,4) gives a sectoring phenotype which disappears once level of Δ NTD becomes 2.5x that of Hsp104 (#5 compared to #2). Sectoring phenotypes were also seen for I14A, Q52A, Y60A/Y62A and R59A, but were not observed for alanine replacements of the DGS loops or modest Y60F/Y62F mutations. Most notable was the strong sectoring of R59A even at expression levels equivalent to chromosomal Hsp104. As was true for Δ NTD, R59A failed to demonstrate a defect in reactivating heat-denatured luciferase (Fig 3b), confirming the prion-specific effect of this residue.

A



B

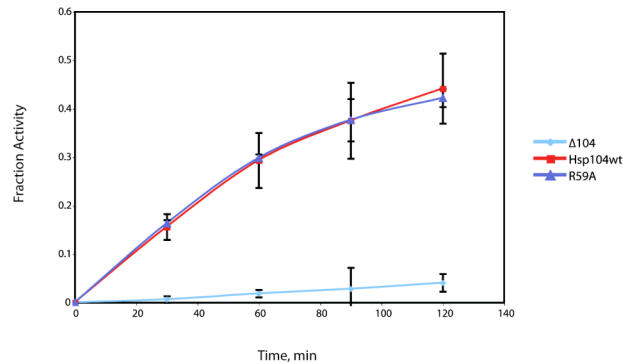
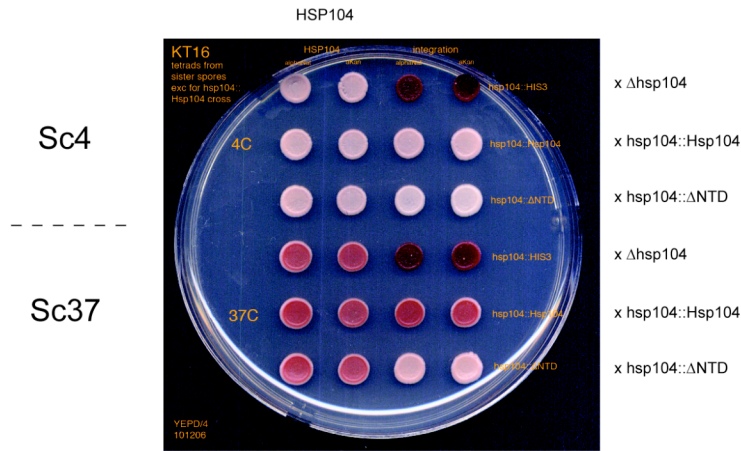


Figure 3. NTD mutant R59A shows a strong [PSI⁺] phenotype but no defect in luciferase refolding. (A) Yeast on low adenine media carrying the allele of Hsp104 indicated in the table to the right from a plasmid shuffle replacement of wild-type Hsp104. All are centromeric plasmids except #1 (chromosomal Hsp104) and #4 (high copy 2 micron plasmid). Above the table is an anti-Hsp104 (Stressgen) Western blot of the indicated yeast strains in log phase. Quantitation of bands relative to the internal control Pgk1 (anti-Pgk1 Invitrogen) and normalized to chromosomal Hsp104 levels are shown in the table. (B) Luciferase assay of R59A as described in Figure 1C.

At this point, I wished to reconstruct my Δ NTD chromosomal replacement and to examine its effect on defined $[PSI^+]$ strains. In an effort to keep expression levels of all alleles equal, I redesigned the promoter-coding region interfaces of my integration construct intermediates and used a wild-type HSP104 integrations allele for a baseline phenotype instead of the completely native HSP104 locus. Integration alleles expressed 10%-20% higher than the native HSP104 allele (data not shown). I replaced Δ hsp104::HIS3 cassettes in yeast with Hsp104-Trp1 or Δ NTD-Trp1 alleles and mated the resulting $[psi^-]$ clones to wild-type $[PSI^+]^{Sc4}$ and $[PSI^+]^{Sc37}$ yeast (Fig 4a). Hsp104-Trp1 alleles weakened $[PSI^+]$ variants slightly due to their slightly higher expression levels than wild-type HSP104. NTD deletion alleles strengthened both $[PSI^+]^{Sc4}$ and, more obviously, $[PSI^+]^{Sc37}$ variants (Fig 4a) but failed to exhibit the sectoring phenotypes seen in previous experiments with episomal Hsp104 alleles and with the original Δ NTD integration.

In order to get a higher-resolution report on the strength of $[PSI^+]$ in the Δ NTD crosses as well as to test an integration of R59A as a representative NTD mutant, I repeated the Hsp104-Trp1 and Δ NTD-Trp1 crosses and performed R59A-Trp1 $[psi^-]$ crosses to $[PSI^+]^{Sc4}$ and $[PSI^+]^{Sc37}$ and examined the resulting phenotypes on trace adenine media. Trace adenine allows more subtle differences in prion variants to be seen. Figure 4b shows parent wild-type $[PSI^+]$ (HSP104 F₀) with a $[psi^-]$ referent above the results of the matings. Frogged from the matings are intermediate diploids and the resulting wild-type (HSP104 F₁) and TRP1-marked allele daughter spores (Fig 4b). For both $[PSI^+]^{Sc4}$ and $[PSI^+]^{Sc37}$, Hsp104-Trp1 weakens the variant as in Figure 4a, but the wild-type sister spore maintains the parental variant through the diploid and sporulation

A



B

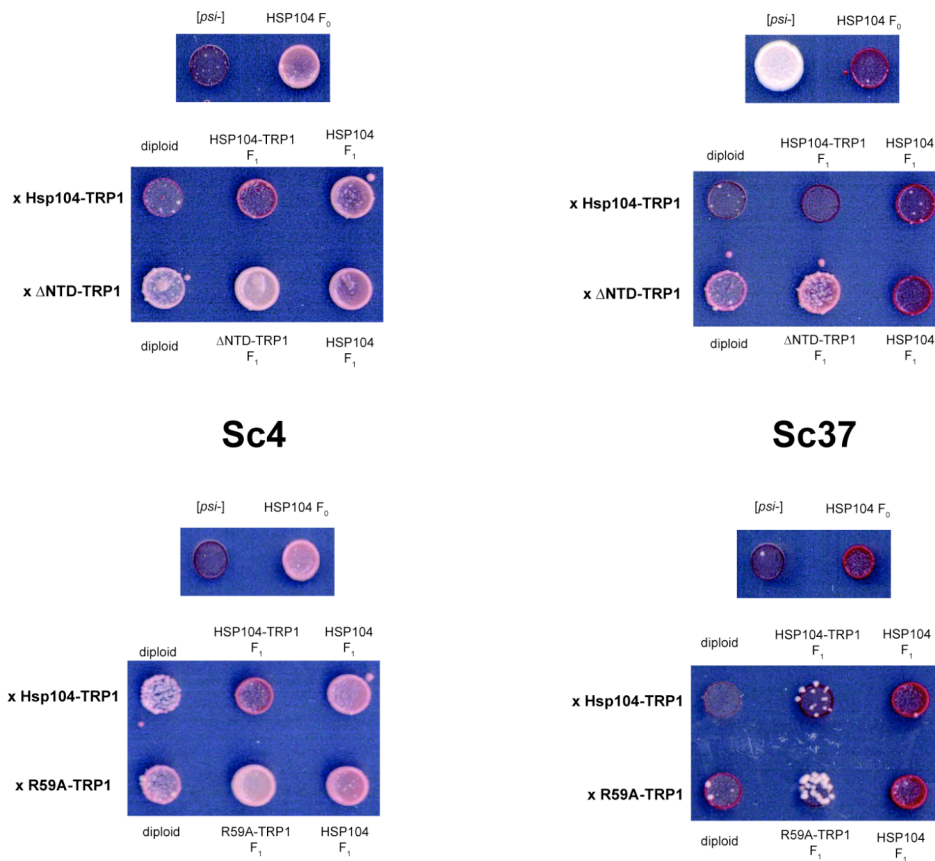


Figure 4. Deletion of NTD strengthens defined variants of $[PSI+]$, but R59A mutation of NTD affects variants differently. (A) Phenotypes of spores on low adenine media resulting from crossing a $[psi-]$ chromosomal TRP1-marked Δ NTD to HSP104 wild-type $[PSI+]^{Sc4}$ (top) and $[PSI+]^{Sc37}$ strains. For each cross, a negative Δ hsp104 and a positive TRP1-marked HSP104 are shown for comparison. Wild-type spores are on the left and Trp+ integration/knockout spores are on the right. (B) Trace adenine media is used to enhance weak $[PSI+]$ phenotypes. Shown are $[psi-]$ and wild-type parent strains above each cross and diploid intermediates with sister wild-type and Hsp104 allele-replacement spores. Crosses to $[PSI+]^{Sc4}$ are on the left and crosses to $[PSI+]^{Sc37}$ are on the right. Cross of Δ NTD-TRP1 with its HSP104-TRP1 reference is on top and cross R59A-TRP1 is on the bottom. Note alteration of phenotype in the diploid stage fails to alter the underlying variant, as all HSP104 spores demonstrate the parental phenotype. All HSP104-TRP1 integrations propagate slightly weaker variants while Δ NTD-TRP1 propagates stronger variants. R59A-TRP1 propagates a stronger Sc4 variant but is unable to maintain the Sc37 variant.

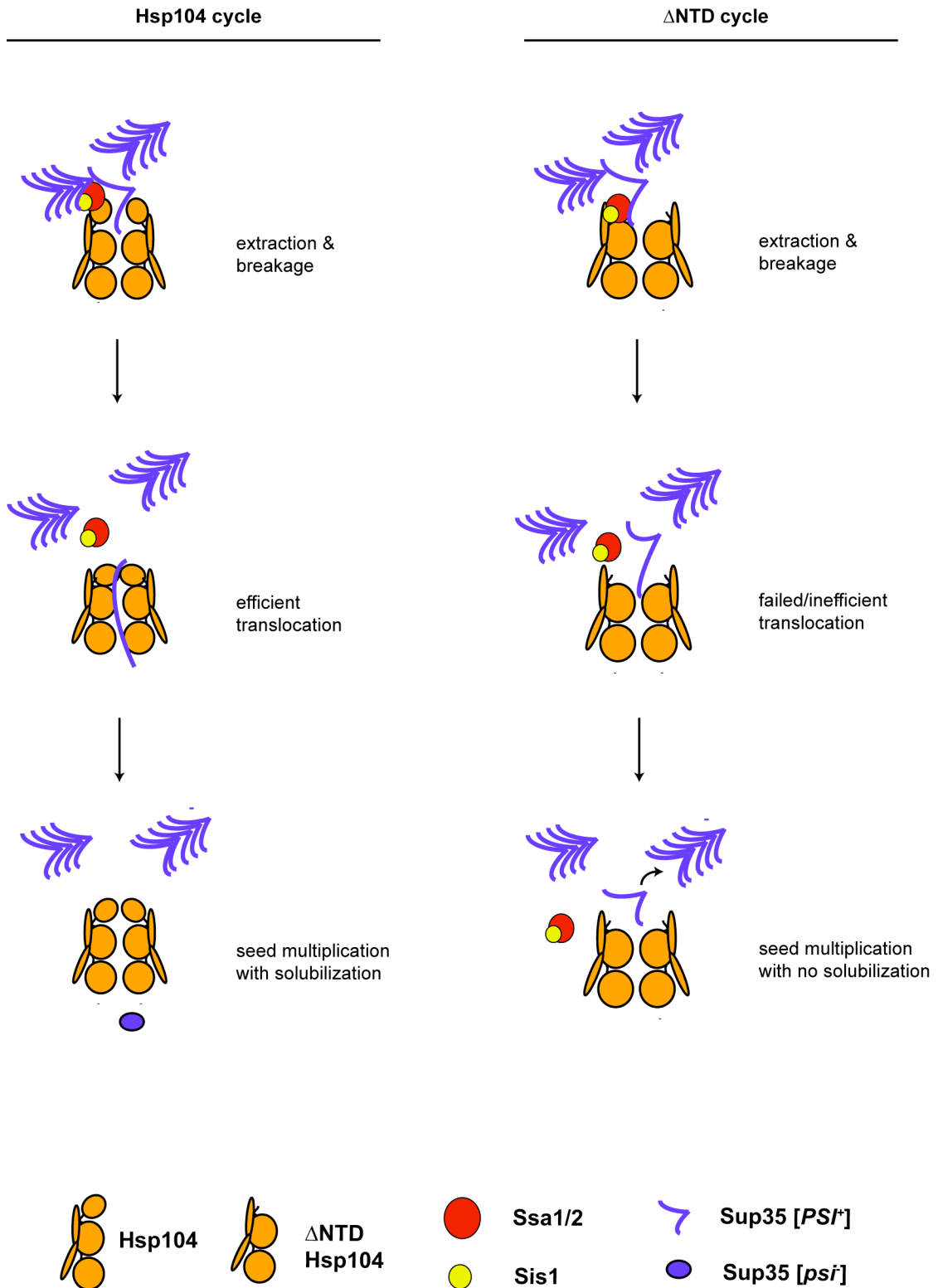
stages. Likewise, Δ NTD-Trp1 strengthens each variant with wild-type sister spores maintaining the parental variant. Interestingly, diploids of HSP104/Hsp104-Trp1 propagated weaker variants than Hsp104/ Δ NTD-Trp1 diploids, indicating mixed ring Hsp104/ Δ NTD hexamers exhibit a phenotype intermediate between pure Hsp104 and pure Δ NTD hexamers. For $[PSI^+]^{Sc4}$, R59A behaved exactly as did Δ NTD, but for $[PSI^+]^{Sc37}$, R59A was unable to maintain the prion. This was the first complete failure of an NTD mutant to maintain a $[PSI^+]$ variant and the first example of a point mutant exhibiting a different phenotype than the domain truncation.

Discussion

My studies of the effect of the NTD on $[PSI^+]$ propagation illustrate the complex relationship of $[PSI^+]$ to Hsp104 levels, but the seemingly disparate results can be interpreted in a cohesive way that results in a model testable by the tools developed during my studies outlined in Chapter 2. Episomally, mutation of or deletion of the NTD resulted in an unstable, stronger variant of $[PSI^+]$. Chromosomally, deletion of the NTD resulted in the same unstable, strong variant of $[PSI^+]$ at expression levels that were about 60-70% of wild-type. However, reduction of levels of Hsp104 full-length the same amount failed to show the $[PSI^+]$ instability phenotype of the Δ NTD (Fig 3a #2). At the higher expression levels (10-20% above wild-type), Hsp104 full-length weakened defined $[PSI^+]$ variants while Δ NTD strengthened defined $[PSI^+]$ variants. In the context of an intact NTD, the point mutation R59A strengthened one variant of $[PSI^+]$ while failing to maintain another. Finally, no NTD mutation or truncation was found to affect Hsp104 functions involving stress-induced aggregates.

The observation that the Hsp104 NTD is dispensable for thermotolerance functions while modulating $[PSI^+]$ variants suggests a gating and processivity role of the NTD in threading substrates through the Hsp104 hexamer. In the absence of the NTD, amorphous aggregates are recruited to Hsp104 and are threaded through the central pore largely as if the NTD were present. Ordered amyloid aggregates, however, are much more stable and may be prone to more “false starts” in Hsp104 action. For these substrates, absence of the NTD would again not affect recruitment and initial engagement of the threading action of Hsp104, but it might affect the efficiency of threading (Fig 5). The end result would be fiber breakage events without complete unfolding, translocation and refolding of monomer, which would explain why increasing amounts of Δ NTD propagate strong prion variants but do not increase the soluble pool of Sup35 protein as full-length Hsp104 does. This model could also account for the failure of R59A to propagate the weaker $[PSI^+]^{Sc37}$ variant, which we know is the result of a physically more rigid fiber type [57] that may have chaperone-recognition sites more obscured than the $[PSI^+]^{Sc4}$ variant [58]. R59A may be able to recognize and engage the more fragile Sc4 fibers but be unable to productively engage Sc37 fibers.

A role for the NTD in gating and processivity is consistent with observations from ClpB biochemical and structural studies and with a very recent study of the Hsp100 ClpX [12]. In this recent study, it was found the successful translocation of substrates through ClpX depended upon ATP turnover rates, which were altered by adaptor interactions with ClpX, and upon the unfolding energy landscape of the substrate protein. Global substrate stability was not necessarily the determinant of whether the Hsp100 could engage but rather whether initial translocation efforts disrupted interactions that were necessary for



native-state folding. If the ATP turnover rates and energy landscape of the substrate were not well-matched for productive engagement, the substrate could escape and refold [12]. ClpB NTD has been shown to bind aggregates [13] and to alter the ATPase cycle of ClpB upon interaction with substrates in a manner dependent upon T7 [62, 65], a residue that is conserved from ClpB to Hsp104 (T8) to *Sp*104 (T7). The crystal structure of TClpB demonstrates a wide range of mobility of the NTD relative to the rest of the molecule that results from the long, flexible linker between NTD and AAA1 [49]. This mobility would be consistent with an opening and closing of the central channel aperture or with an allosteric action that could affect ATP turnover. Interference with coordinated motion of the NTD through the flexible linker might explain frequency of the mutation in T160 in my and the Masison lab's screens (T160R twice in my screen, T160M in Masison screen). T160 lies within the linker sequence and is conserved in budding yeast but diverges in fission yeast.

My mutational studies of the NTD were limited by the complexity and sensitivity to chaperone levels of the relationship of Hsp104 and [*PSI*⁺]. The tools I developed in my studies outlined in Chapter 2, however, open up many new experimental avenues for assessing the effects of the NTD truncation and mutants. A clear prediction of my model for NTD function is to test the flux of Sup35 through Δ NTD_4BAP, 4BAP R59A and 4BAP T160R in different [*PSI*⁺] variants. Unlike with Hsp104, propagation may not result in Sup35 trapping in the absence of the NTD. If this were the case, the implication would be that translocation occurs simultaneously with amyloid fragmentation but is not strictly necessary for prion propagation.

Materials & Methods

Strains and Plasmids

Plasmids were constructed by standard cloning techniques using a modular, restriction enzyme-delineated promoter-coding region-utr structure. All plasmids assaying Hsp104 function were under the control of the native HSP104 promoter. Early constructs used (Fig 1b, Fig 3a & b) replaced the HSP104 Kozak sequence with a BamHI site. Later constructs (Fig 1c, Fig 4 integrations) inserted the BamHI site after the native Kozak. Integration constructs were constructed by homologous recombination, transforming Δ hsp104::HIS3 yeast with DNA fragments of the following composition:

HSP104promoter-coding region-150bp 3'utr-TRP1-3'utr homology151-250.

Transformants were selected on –Trp media, confirmed to be His auxotrophs, and chromosomal placement was confirmed by PCR.

Luciferase Refolding

These assays were performed exactly as described in Chapter 2 methods.

Random Mutagenesis

Stratagene GeneMorph II mutagenesis kit was used to mutagenize residues -100 to 835 of Hsp104 on a carrier plasmid with a SnaBI site silently inserted at nucleotide 578, 3' of the NTD. The mutant library was constructed by subcloning BamHI/SnaBI fragments from the mutagenized DNA into p315hsHsp104 BamHI/SnaBI. Trial sequencing confirmed an average mutation rate of 1 per fragment. Mutants were introduced into

[*PSI*⁺] Δ hsp104 yeast carrying a URA-marked plasmid with Hsp104 under its native promoter by standard transformation and selected on SD-Ura-Leu, then passaged on SD-Leu, 5-FOA to lose the wildtype Hsp104 plasmid, then on SD-Leu, low adenine. Sectoring candidates were chosen and sequenced by colony PCR.

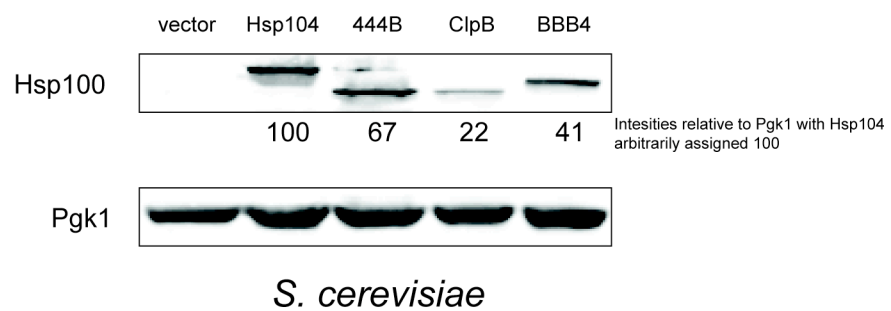
Structure-based mutagenesis

Alignments were conducted using CLUSTAL-W in MacVector or using Toffee. Clement's structure was viewed using SwissPDB Viewer and Mac PyMol. Selected residues were mutated using QuikChange technology and confirmed by sequencing.

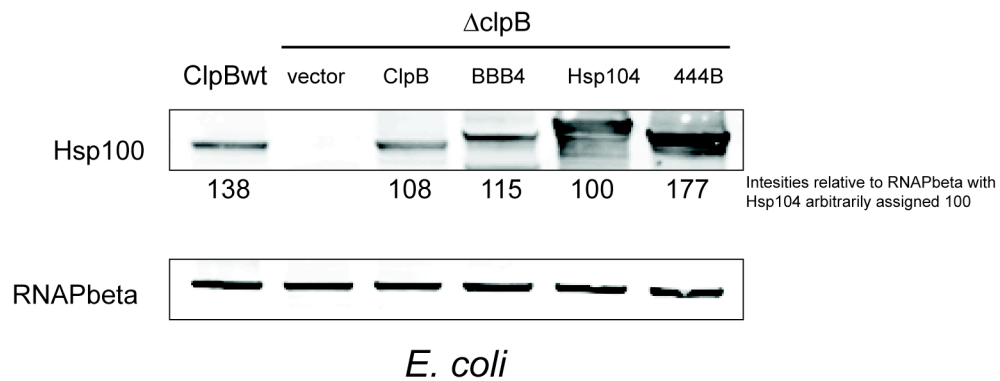
Appendix A

Chapter 2 Supplemental Figures

A

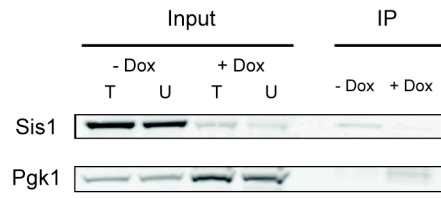


B

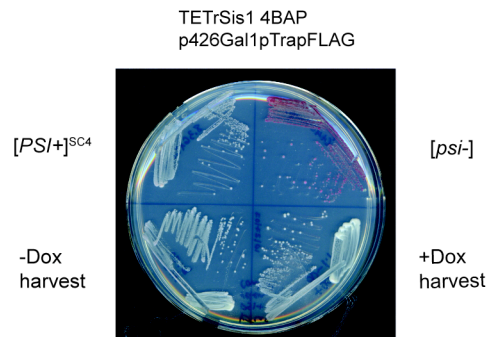


A

IP: α -FLAG
IB: α -Sis1, α -Pgk1



B



C

IP: α -FLAG
IB: α -Sis1, α -Pgk1



Appendix A: Figure Legends

Figure 1. Expression Levels of Hsp100s in yeast and bacteria. Cultures of (A) yeast or (B) bacteria expressing the indicated Hsp100 were exposed to mild heat shock to induce Hsp100 expression and harvested. Cleared lysates of cells were submitted to SDS-PAGE, transferred to nitrocellulose and probed with a mixture of ClpB-reactive and Hsp104NTD-reactive antibodies plus antibodies reactive to abundant soluble proteins as an internal loading control (Pgk1 in yeast, RNAPbeta (RNA polymerase beta subunit) in bacteria). Fresh preparations of the same ratio of anti-ClpB/anti-Hsp104NTD were used for each blot to enable comparison of the ratio of Hsp100 expressed if not the absolute amount.

Figure 2. Sis1 inhibition reduces translocation of prion proteins from their aggregate substrates. (A) and (C) Blots from Chapter 2, Figure 5b were probed for Sis1 and Pgk1. The decrease in Sis1 levels was determined by analysis using the LiCor Odyssey densitometry software. The abundant soluble protein Pgk1 failed to immunoprecipitate, confirming the specificity of the elution signals. (B) Harvest cultures for Sis1 shutoff experiment in Chapter 2, Figure 5b left. The doxycycline treatment, which resulted in a 12-fold decrease in Sup35 translocation, was insufficient to cure the cells of [*PSI*⁺].

Appendix B

Hsp104/ClpB chimera function in yeast

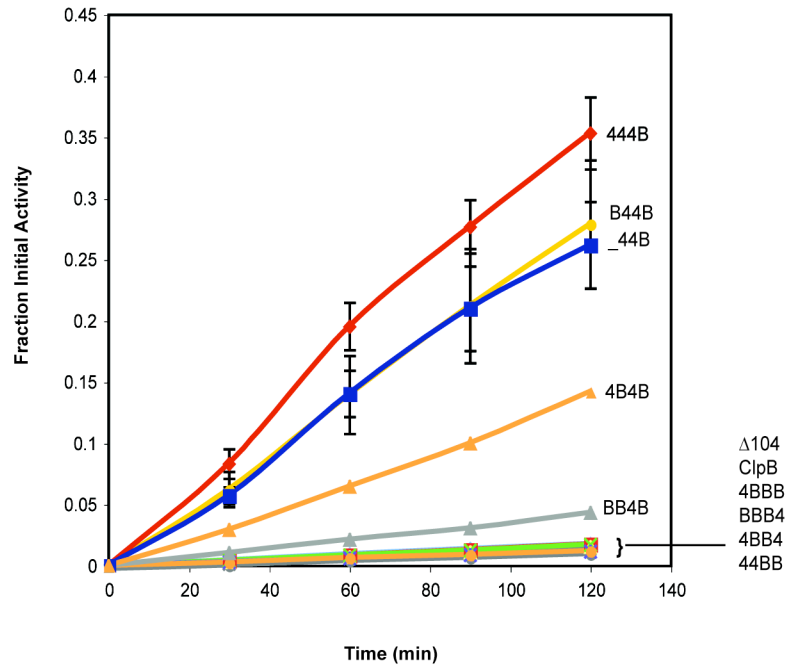
This appendix reports some interesting and somewhat unexpected results from Hsp104/ClpB chimeras not discussed in Chapter 2. The functioning in Hsp70/40-dependent reactions of 444B in yeast and BBB4 in bacteria demonstrated the lack of specific coupling of the AAA2 to the particular cellular environment for these reactions. These same reactions were independent of the presence or absence of the ClpB NTD or the Hsp104 NTD in the context of the native chaperone, as shown in previous literature [61, 64] and in Chapter 3. By elimination, that left the AAA1 and CC domains as candidates for conveying specificity in Hsp100 interaction with Hsp70/40 and therefore in thermotolerance and $[PSI^+]$ propagation reactions. The remaining question was whether AAA1 was a generic module and CC a specific one as might be expected from their respective degrees of evolutionary conservation and divergence among Hsp100 homologs.

I began treating the AAA1+CC as a single module based upon close contacts between the two in structural studies of *T*ClpB [49]. These contacts were later found to alter with the ATPase cycle of ClpB [35]. Further, the CC domain was found to couple the initial DnaK-dependent steps of disaggregation to ClpB translocation motor activity [44]. This DnaK-dependent initial step results in binding of substrates to AAA1 [40]. All of these studies indicate that CC and AAA1 domains are intimately connected functionally as well as structurally. Therefore, even if part of the CC had coevolved with other cellular machinery to achieve diversity, it would be difficult to show due to its coevolution with the specific AAA1 as well. However, I tried to dissect them in my Hsp104/ClpB chimera studies for the sake of completeness. These studies were restricted to yeast.

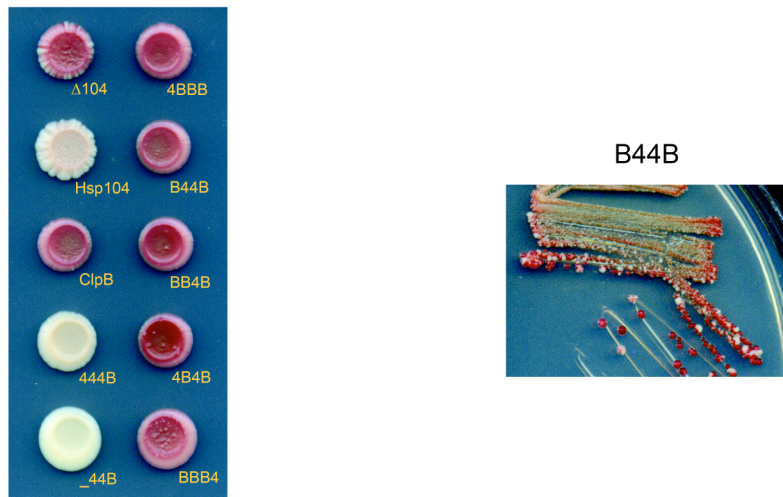
The chimeras I constructed and tested for luciferase refolding and [PSI^+] propagation were the originals, 444B and BBB4, the N-terminal truncation of 444B ($_44B$) and the series expected to be negative controls: 4BBB, 4BB4, 44BB, B44B, 4B4B and BB4B. Testing these constructs *in vivo* in luciferase refolding (Fig A), performed as described in Chapter 2, I found that 4BBB, 4BB4 and 44BB were completely inactive, as would be expected from the AAA1-CC module BB in the first two and from the mixed AAA1-CC module 4B in the last. The N-terminal truncation of 444B, $_44B$ was functional in luciferase refolding, although it performed about 25% worse than 444B. This is in contrast to the complete functioning of Δ NTD compared to Hsp104 in the same assay (Chapter 3, Fig 1C). Substitution of Hsp104 NTD with ClpB NTD to form B44B had the same effect as the truncation of NTD. Most interestingly, BB4B has a low but convincingly above null level of activity and 4B4B showed activity at around 30% of 444B. These constructs were not at all expected to work due to their chimera AAA1-CC construction of B4.

Next, I wished to test the ability of these constructs to propagate [PSI^+]. Using the same assay described in Chapter 2, Figure 2, I found that $_44B$ was able to propagate [PSI^+] (FigB, left) and, surprisingly B44B was able to propagate [PSI^+], although with a severe defect (Fig B, right). As with Δ NTD and Hsp104, elimination of the NTD of 444B strengthened the [PSI^+] phenotype. Given the model I proposed at the end of Chapter 3, I interpreted the ability of B44B to propagate a very unstable [PSI^+] as the deleterious but not completely inhibitory effect of gating the Hsp100 pore with a domain unable to recognize [PSI^+] aggregates.

A



B



Overall, the results of these experiments support the idea that AAA1 and CC cooperate and must come from the same molecule to function well. Only chimeras with Hsp104 AAA1 and CC domains were able to handle the stable, ordered aggregates of $[PSI^+]$. Consistent with my studies in Chapter 3, loss of the NTD in this context strengthened $[PSI^+]$ and substitution of the NTD with a “defective” counterpart, like R59A for $[PSI^+]^{Sc37}$, interfered with functioning. Interestingly, this was not true for luciferase refolding. This makes sense, though, in that either ClpB or Hsp104 can refold luciferase, the Hsp70/40 contribution seems to be mediated through AAA1 and CC [35, 40, 44], and the NTD is a discrete domain on a relatively long tether unlikely to have many intimate, coevolved contacts with AAA1 and CC [49]. The real surprise is the functioning of 4B4B. The fact that this molecule works at all in yeast supports the idea that the NTD and CC are accessory domains on the generic barrel of AAA1-AAA2 and that are dependent upon the specific cellular context for their contributions to function. Also, this molecule shows that the specific coupling of AAA1 and CC is not absolutely necessary for functioning.

The set of Hsp104/ClpB chimeras I have built to study the interaction of Hsp104 with its co-chaperones and substrates in yeast show the degree to which these molecules are modular constructions. Continued study of these molecules, especially *in vitro*, will allow a more precise dissection of ClpB/Hsp104 reaction mechanisms. In particular, they may serve as productive tools in studying the co-evolution of cellular chaperones with each other and with their substrates.

Materials & Methods

All constructs and assays are essentially as described in Chapter 2. Chimeras were constructed by fusion PCR and cloned into p315 under the control of the HSP104 promoter and with 150bp of the HSP104 3'utr. Luciferase assays used pGPDlux, kindly provided by B. Bukau.

Appendix C

Hsp104-containing extracts sever Sup35NM fibers

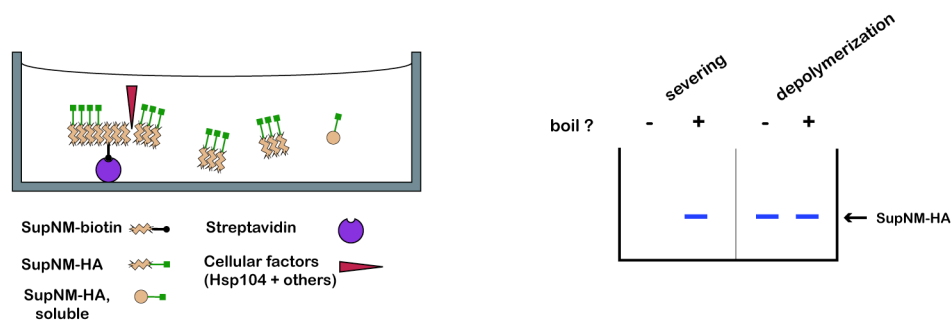
Hsp104 is known to be required for prion replication in yeast [4], and this activity has been proposed to be a fragmentation of amyloid aggregates to expose new ends for growth [6]. Despite published reports of activity of Hsp104 alone on SupNM fiber substrates [7], my and other efforts in our lab failed to reproduce this activity. My subsequent studies *in vivo* detailed in Chapter 2 provide an explanation for this failure: Hsp104 is reliant upon Sis1 and probably Ssa1 to act on Sup35 fiber substrates. This assay was an attempt at a top-down approach to identifying factors necessary for Sup35 fiber fragmentation. It was somewhat successful but was not sensitive enough or of high enough resolution for our needs. Nevertheless, I saw Hsp104-dependent release of fiber fragments from SupNM aggregate substrates, a result that was confirmed in a separate study from Masasuke Yoshida's lab [5].

Shown in Figure A is a schematic of the prion replication assay I developed. Recombinant Sup35NM, tagged with the HA epitope, was polymerized from preformed seeds of SupNM-HA56 (unable to react to anti-HA antibody) and SupNM-biotin. Fibers were bound to streptavidin-coated wells in 96-well plates and yeast extracts from wild-type or Δ hsp104 yeast was added. Aliquots were removed at 10-15 minute time intervals, split and either boiled or not boiled before separation by SDS-PAGE. Samples were transferred to nitrocellulose and probed with anti-HA antibody. Monomeric SupNM-HA would be expected to migrate into the gel with or without boiling, while aggregated SupNM-HA would be expected to migrate into the gel only upon boiling.

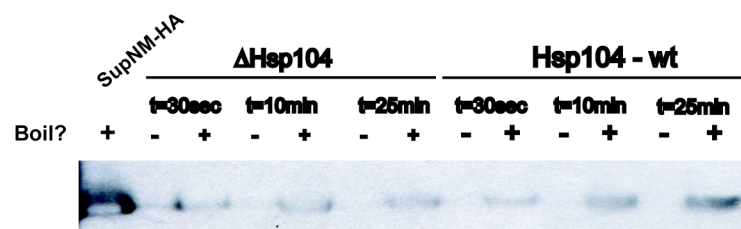
Shown in Figure B is data generated using the experimental schematic outlined in Figure A. Over a period of 25 minutes, extracts containing Hsp104 released SDS-

A

Prion Replication Assay



B



resistant Sup35 fiber fragments but no detectable Sup35 monomer. Later experiments showed this activity could be halted by addition of the divalent cation chelator EDTA.

Materials and Methods

SupNM, SupNM-HA, SupNM-cys was purified and polymerized according to standard Weissman lab protocols [66] using 10% seed containing 20% biotinylated Sup35. Streptavidin plates were Nunc #436020. Polymerized fibers were bound for 60 minutes to streptavidin plates prewashed with PBST. Unbound fibers were removed and wells were washed 3x PBST. Yeast extracts at ~2.5 mg/mL were added with Roche Complete Protease inhibitors, 5mM ATP, creatine kinase and creatine phosphate and plates were incubated at 30°C. Aliquots were removed at 10-15 minute time intervals and analyzed by SDS-PAGE and Western Blot. Extract prep protocol below.

Yeast Extract Prep: ATPase Activity

1. 50mL ON in YEPD
2. Dilute to $OD_{600} = 0.15$ in 250mL YEPD
3. At $OD_{600} = 0.6-0.8$, pellet cells (4800rpm on big rotor 15 min) and resuspend in Resuspension Buffer. Incubate at RT 5min.
4. Pellet cells and resuspend in 5mL Spheroplasting buffer. Take OD_{600} by adding 10uL cells to 1mL ddH₂O. Add Lyticase and incubate at 30°C 30min or until >90% of cells are spheroplasted as indicated by 1:100 OD_{600} in ddH₂O.
5. Pellet spheroplasts (2500 rpm/1250g 6min); Wash gently in Wash Buffer.
6. Resuspend spheroplasts w/ yellow tip to ensure greater lysis in 2.5mL Hypotonic Lysis Buffer + DTT + ATP.
7. Incubate on ice 10min. Add NaCl to 100mM.
8. Spin lysate for 10min at 3220g (4K rpm). Take sup and repeat spin.

9. Measure total protein yield by Bradford/BioRad and freeze aliquots in liquid N₂. Store at -80.

Buffers

add DTT (1M stock), lyticase, ATP (100mM stock) and Roche EDTA-free protease inhibitors on day of use. Roche prot inhib can be stored as 10X stock in lysis buffer w/out ATP in 4°C.

Resuspension Buffer: 100mM Tris, pH9.4
10mM DTT

Spheroplasting Buffer: 0.7M Sorbitol
10mM Tris, pH 7.5
100mM NaCl
1mM DTT
10mM NaN₃ and NaF
0.5mL Lyticase per 5mL total

Wash Buffer: 0.7M Sorbitol
50mM Na₂PO₄, pH 7.0

Hypotonic Lysis Buffer: 10mM NaCl
25mM Na₂PO₄, pH 7.0
1mM EDTA
0.1% Triton X-100
+ 1mM ATP
+ 1X protease inhibitors

Protease inhibitor: Roche Complete EDTA-free (1 873 580)
1 tablet per 5mL Lysis buffer for 10X stock.

Appendix D

References

1. Chiti, F. and C.M. Dobson, *Protein misfolding, functional amyloid, and human disease*. Annu Rev Biochem, 2006. **75**: p. 333-66.
2. Wickner, R.B., *[URE3] as an altered URE2 protein: evidence for a prion analog in Saccharomyces cerevisiae*. Science, 1994. **264**(5158): p. 566-9.
3. Osherovich, L.Z., et al., *Dissection and design of yeast prions*. PLoS Biol, 2004. **2**(4): p. E86.
4. Chernoff, Y.O., et al., *Role of the chaperone protein Hsp104 in propagation of the yeast prion-like factor [psi+]*. Science, 1995. **268**(5212): p. 880-4.
5. Inoue, Y., et al., *Hsp104 binds to yeast Sup35 prion fiber but needs other factor(s) to sever it*. J Biol Chem, 2004. **279**(50): p. 52319-23.
6. Paushkin, S.V., et al., *Propagation of the yeast prion-like [psi+] determinant is mediated by oligomerization of the SUP35-encoded polypeptide chain release factor*. Embo J, 1996. **15**(12): p. 3127-34.
7. Shorter, J. and S. Lindquist, *Hsp104 catalyzes formation and elimination of self-replicating Sup35 prion conformers*. Science, 2004. **304**(5678): p. 1793-7.
8. Lee, S., et al., *The ClpB/Hsp104 molecular chaperone-a protein disaggregating machine*. J Struct Biol, 2004. **146**(1-2): p. 99-105.
9. Mogk, A., et al., *Common and specific mechanisms of AAA+ proteins involved in protein quality control*. Biochem Soc Trans, 2008. **36**(Pt 1): p. 120-5.
10. Kenniston, J.A., et al., *Linkage between ATP consumption and mechanical unfolding during the protein processing reactions of an AAA+ degradation machine*. Cell, 2003. **114**(4): p. 511-20.
11. Kenniston, J.A., et al., *Effects of local protein stability and the geometric position of the substrate degradation tag on the efficiency of ClpXP denaturation and degradation*. J Struct Biol, 2004. **146**(1-2): p. 130-40.
12. Martin, A., T.A. Baker, and R.T. Sauer, *Protein unfolding by a AAA+ protease is dependent on ATP-hydrolysis rates and substrate energy landscapes*. Nat Struct Mol Biol, 2008. **15**(2): p. 139-45.
13. Barnett, M.E., et al., *The amino-terminal domain of ClpB supports binding to strongly aggregated proteins*. J Biol Chem, 2005. **280**(41): p. 34940-5.
14. Thibault, G., et al., *Specificity in substrate and cofactor recognition by the N-terminal domain of the chaperone ClpX*. Proc Natl Acad Sci U S A, 2006. **103**(47): p. 17724-9.
15. Xia, D., et al., *Crystallographic investigation of peptide binding sites in the N-domain of the ClpA chaperone*. J Struct Biol, 2004. **146**(1-2): p. 166-79.
16. Zeth, K., et al., *Structural analysis of the adaptor protein ClpS in complex with the N-terminal domain of ClpA*. Nat Struct Biol, 2002. **9**(12): p. 906-11.
17. Muchowski, P.J. and J.L. Wacker, *Modulation of neurodegeneration by molecular chaperones*. Nat Rev Neurosci, 2005. **6**(1): p. 11-22.
18. King, C.Y. and R. Diaz-Avalos, *Protein-only transmission of three yeast prion strains*. Nature, 2004. **428**(6980): p. 319-23.
19. Tanaka, M., et al., *Conformational variations in an infectious protein determine prion strain differences*. Nature, 2004. **428**(6980): p. 323-8.
20. Kryndushkin, D.S., et al., *Yeast [PSI+] prion aggregates are formed by small Sup35 polymers fragmented by Hsp104*. J Biol Chem, 2003. **278**(49): p. 49636-43.
21. Shorter, J. and S. Lindquist, *Destruction or potentiation of different prions catalyzed by similar Hsp104 remodeling activities*. Mol Cell, 2006. **23**(3): p. 425-38.
22. Zhou, P., I.L. Derkatch, and S.W. Liebman, *The relationship between visible intracellular aggregates that appear after overexpression of Sup35 and the yeast prion-like elements [PSI(+)] and [PIN(+)]*. Mol Microbiol, 2001. **39**(1): p. 37-46.
23. Jones, G.W. and M.F. Tuite, *Chaperoning prions: the cellular machinery for propagating an infectious protein?* Bioessays, 2005. **27**(8): p. 823-32.
24. Osherovich, L.Z. and J.S. Weissman, *The utility of prions*. Dev Cell, 2002. **2**(2): p. 143-51.

25. Jung, G., et al., *A role for cytosolic hsp70 in yeast [PSI(+)] prion propagation and [PSI(+)] as a cellular stress*. Genetics, 2000. **156**(2): p. 559-70.
26. Jones, G., et al., *Propagation of Saccharomyces cerevisiae [PSI+] prion is impaired by factors that regulate Hsp70 substrate binding*. Mol Cell Biol, 2004. **24**(9): p. 3928-37.
27. Jones, G.W. and D.C. Masison, *Saccharomyces cerevisiae Hsp70 mutations affect [PSI+] prion propagation and cell growth differently and implicate Hsp40 and tetra-tryptophan repeat cochaperones in impairment of [PSI+]*. Genetics, 2003. **163**(2): p. 495-506.
28. Loovers, H.M., E. Guinan, and G.W. Jones, *Importance of the Hsp70 ATPase domain in yeast prion propagation*. Genetics, 2007. **175**(2): p. 621-30.
29. Song, Y., et al., *Role for Hsp70 chaperone in Saccharomyces cerevisiae prion seed replication*. Eukaryot Cell, 2005. **4**(2): p. 289-97.
30. Allen, K.D., et al., *Hsp70 chaperones as modulators of prion life cycle: novel effects of Ssa and Ssb on the Saccharomyces cerevisiae prion [PSI+]*. Genetics, 2005. **169**(3): p. 1227-42.
31. Luke, M.M., A. Sutton, and K.T. Arndt, *Characterization of SISI, a Saccharomyces cerevisiae homologue of bacterial dnaJ proteins*. J Cell Biol, 1991. **114**(4): p. 623-38.
32. Sondheimer, N., et al., *The role of Sis1 in the maintenance of the [RNQ+] prion*. Embo J, 2001. **20**(10): p. 2435-42.
33. Aron, R., et al., *J-protein co-chaperone Sis1 required for generation of [RNQ+] seeds necessary for prion propagation*. Embo J, 2007. **26**(16): p. 3794-803.
34. White, S.R. and B. Lauring, *AAA+ ATPases: achieving diversity of function with conserved machinery*. Traffic, 2007. **8**(12): p. 1657-67.
35. Lee, S., J.M. Choi, and F.T. Tsai, *Visualizing the ATPase cycle in a protein disaggregating machine: structural basis for substrate binding by ClpB*. Mol Cell, 2007. **25**(2): p. 261-71.
36. Glover, J.R. and S. Lindquist, *Hsp104, Hsp70, and Hsp40: a novel chaperone system that rescues previously aggregated proteins*. Cell, 1998. **94**(1): p. 73-82.
37. Parsell, D.A., et al., *Protein disaggregation mediated by heat-shock protein Hsp104*. Nature, 1994. **372**(6505): p. 475-8.
38. Motohashi, K., et al., *Heat-inactivated proteins are rescued by the DnaK.J-GrpE set and ClpB chaperones*. Proc Natl Acad Sci U S A, 1999. **96**(13): p. 7184-9.
39. Zolkiewski, M., *ClpB cooperates with DnaK, DnaJ, and GrpE in suppressing protein aggregation. A novel multi-chaperone system from Escherichia coli*. J Biol Chem, 1999. **274**(40): p. 28083-6.
40. Weibezahn, J., et al., *Thermotolerance requires refolding of aggregated proteins by substrate translocation through the central pore of ClpB*. Cell, 2004. **119**(5): p. 653-65.
41. Zietkiewicz, S., J. Krzewska, and K. Liberek, *Successive and synergistic action of the Hsp70 and Hsp100 chaperones in protein disaggregation*. J Biol Chem, 2004. **279**(43): p. 44376-83.
42. Zietkiewicz, S., et al., *Hsp70 chaperone machine remodels protein aggregates at the initial step of Hsp70-Hsp100-dependent disaggregation*. J Biol Chem, 2006. **281**(11): p. 7022-9.
43. Schlee, S., et al., *A chaperone network for the resolubilization of protein aggregates: direct interaction of ClpB and DnaK*. J Mol Biol, 2004. **336**(1): p. 275-85.
44. Haslberger, T., et al., *M domains couple the ClpB threading motor with the DnaK chaperone activity*. Mol Cell, 2007. **25**(2): p. 247-60.
45. Bosl, B., V. Grimminger, and S. Walter, *The molecular chaperone Hsp104--a molecular machine for protein disaggregation*. J Struct Biol, 2006. **156**(1): p. 139-48.
46. Krzewska, J., T. Langer, and K. Liberek, *Mitochondrial Hsp78, a member of the Clp/Hsp100 family in Saccharomyces cerevisiae, cooperates with Hsp70 in protein refolding*. FEBS Lett, 2001. **489**(1): p. 92-6.
47. Flynn, J.M., et al., *Proteomic discovery of cellular substrates of the ClpXP protease reveals five classes of ClpX-recognition signals*. Mol Cell, 2003. **11**(3): p. 671-83.
48. Tessarz, P., A. Mogk, and B. Bukau, *Substrate threading through the central pore of the Hsp104 chaperone as a common mechanism for protein disaggregation and prion propagation*. Mol Microbiol, 2008. **68**(1): p. 87-97.
49. Lee, S., et al., *The structure of ClpB: a molecular chaperone that rescues proteins from an aggregated state*. Cell, 2003. **115**(2): p. 229-40.
50. Iyer, L.M., et al., *Evolutionary history and higher order classification of AAA+ ATPases*. J Struct Biol, 2004. **146**(1-2): p. 11-31.

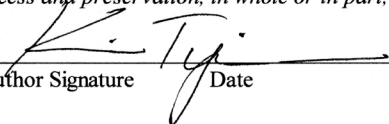
51. Mogk, A., et al., *Roles of individual domains and conserved motifs of the AAA+ chaperone ClpB in oligomerization, ATP hydrolysis, and chaperone activity.* J Biol Chem, 2003. **278**(20): p. 17615-24.
52. Schirmer, E.C., et al., *Subunit interactions influence the biochemical and biological properties of Hsp104.* Proc Natl Acad Sci U S A, 2001. **98**(3): p. 914-9.
53. Bosl, B., V. Grimminger, and S. Walter, *Substrate binding to the molecular chaperone Hsp104 and its regulation by nucleotides.* J Biol Chem, 2005. **280**(46): p. 38170-6.
54. Abbas-Terki, T., et al., *Hsp104 interacts with Hsp90 cochaperones in respiring yeast.* Mol Cell Biol, 2001. **21**(22): p. 7569-75.
55. Ross, E.D., U. Baxa, and R.B. Wickner, *Scrambled prion domains form prions and amyloid.* Mol Cell Biol, 2004. **24**(16): p. 7206-13.
56. Shewmaker, F., et al., *Amyloids of Shuffled Prion Domains That Form Prions Have a Parallel In-Register beta-Sheet Structure.* Biochemistry, 2008.
57. Tanaka, M., et al., *The physical basis of how prion conformations determine strain phenotypes.* Nature, 2006. **442**(7102): p. 585-9.
58. Toyama, B.H., et al., *The structural basis of yeast prion strain variants.* Nature, 2007. **449**(7159): p. 233-7.
59. Sanchez, Y. and S.L. Lindquist, *HSP104 required for induced thermotolerance.* Science, 1990. **248**(4959): p. 1112-5.
60. Michelitsch, M.D. and J.S. Weissman, *A census of glutamine/asparagine-rich regions: implications for their conserved function and the prediction of novel prions.* Proc Natl Acad Sci U S A, 2000. **97**(22): p. 11910-5.
61. Beinker, P., et al., *The N terminus of ClpB from Thermus thermophilus is not essential for the chaperone activity.* J Biol Chem, 2002. **277**(49): p. 47160-6.
62. Liu, Z., et al., *Conserved amino acid residues within the amino-terminal domain of ClpB are essential for the chaperone activity.* J Mol Biol, 2002. **321**(1): p. 111-20.
63. Chow, I.T., et al., *The N-terminal domain of Escherichia coli ClpB enhances chaperone function.* FEBS Lett, 2005. **579**(20): p. 4242-8.
64. Hung, G.C. and D.C. Masison, *N-terminal domain of yeast Hsp104 chaperone is dispensable for thermotolerance and prion propagation but necessary for curing prions by Hsp104 overexpression.* Genetics, 2006. **173**(2): p. 611-20.
65. Li, J. and B. Sha, *Crystal structure of the E. coli Hsp100 ClpB N-terminal domain.* Structure (Camb), 2003. **11**(3): p. 323-8.
66. DePace, A.H., et al., *A critical role for amino-terminal glutamine/asparagine repeats in the formation and propagation of a yeast prion.* Cell, 1998. **93**(7): p. 1241-52.

Publishing Agreement

It is the policy of the University to encourage the distribution of all theses and dissertations. Copies of all UCSF theses and dissertations will be routed to the library via the Graduate Division. The library will make all theses and dissertations accessible to the public and will preserve these to the best of their abilities, in perpetuity.

Please sign the following statement:

I hereby grant permission to the Graduate Division of the University of California, San Francisco to release copies of my thesis or dissertation to the Campus Library to provide access and preservation, in whole or in part, in perpetuity.

 March 30, 2008
Author Signature Date